IMPACT OF SUBSURFACE HETEROGENEITY STRUCTURE ON CONTAMINANT TRANSPORT: A ONE-DIMENSIONAL CASE

A Thesis

by

SHUO YANG

Submitted to the Office of Graduate and Professional Studies of
Texas A&M University
in partial fulfillment of the requirements for the degree of

MASTER OF SCIENCE

Chair of Committee,	Hongbin Zhan
Committee Members,	Peter Knappett
	David Sparks
Head of Department,	Michael Pope

December 2017

Major Subject: Geology

ABSTRACT

Influence of heterogeneity on subsurface contaminant transport is one of the most important and challenging tasks in contaminant hydrogeology, and it often requires a stochastic approach that is found to be difficult to apply in real-world problems. This thesis adopts a simple analytical approach to investigate the influence of heterogeneity structure on contaminant transport in a one-dimensional setting. Compared with numerical models, analytical treatment is more commonly used for this issue, since it is straightforward to apply and is free from numerical problems such as numerical dispersion and artificial oscillation. This thesis assumes that Fickian dispersion is valid and uses the advection-dispersion equation (ADE) as the governing equation for studying one-dimensional contaminant transport in a heterogeneous system consisting of two zones with different transport properties, first-order reaction and linear sorption. The governing equation is solved in Laplace domain and the solution is obtained in real-time domain using a numerical inverse Laplace transform program named the de Hoog algorithm. A MATLAB program is created to facilitate the computation. Through analyzing several conceptual cases, the results of this research reflect that: (1) The order of heterogeneity will affect the contaminant transport in the two-zone porous media; (2) The difference of transport properties will affect the contaminant transport results when the order of heterogeneity reverses; (3) The accuracy of parameter homogenization will decrease with the increasing difference between parameters of the two zones. The homogenized parameter values will depend on the order of heterogeneity; (4) Dispersivity has the greatest influence on the

results of BTCs and it is also the most difficult one to be homogenized. The accuracy of homogenization of dispersivity is scale-dependency; and (5) When there are multiple parameters to be homogenized simultaneously, the homogenized solutions may be out of the range bonded by the parameter of two zones. This research is expected to fill the gap of subsurface heterogeneity structure influence on solute migration in two-zone porous media.

ACKNOWLEDGEMENTS

I appreciate my committee chair, Dr. Zhan, and my committee members, Dr. Knappett, and Dr. Sparks, for their guidance and suggestions about my research that helped to improve my thesis.

I would like to thank Dr. Liang for helping me develop the MATLAB script for fitting curve, and Hollenbeck for providing a copy of the MATLAB code of numerical inversion by the de Hoog method.

Thanks also to my family and friends Xin Liu and Renjie Zhou for their support and encouragement throughout writing this thesis.

CONTRIBUTORS AND FUNDING SOURCES

Contributors

This work was supervised by a thesis committee consisting of Dr. Hongbin Zhan, and Dr. David Sparks of the Department of Geology & Geophysics and Dr. Peter Knappett of the Department of Water Management & Hydrological Science.

All other work conducted for the thesis was completed by the student.

Funding Sources

There are no outside funding contributions to the research and compilation of this thesis.

NOMENCLATURE

q	Darcy velocity, (m/day).
v	Average pore velocity, (m/day).
v_1, v_2	Average pore velocities of zone-1 and zone-2, respectively (m/day).
t	Time, (day).
R	Retardation factor.
R_1, R_2	Retardation factors of zone-1 and zone-2, respectively.
α	Longitudinal dispersivity, (m).
α_1 , α_2	Longitudinal dispersivities of zone-1 and zone-2, respectively (m).
D	Dispersion coefficient, (m^2/day).
D_1, D_2	Dispersion coefficients of zone-1 and zone-2, respectively (m^2/day).
θ	Porosity.
θ_1 , θ_2	Porosities of zone-1 and zone-2, respectively.
λ	Reaction rate, (1/day).
λ_1 , λ_2	Reaction rates of zone-1 and zone-2, respectively (1/day).
L_1	Length of zone-1, (m).
L	The total length of zone-1 and zone-2, (m).
C	Concentration of adsorbate in solution, (mg/L).
C_0	Initial concentration outside of the inlet boundary, (mg/L).

C_1, C_2	Concentrations of the adsorbate in solution of zone-1 and zone-2, respectively (mg/L).
$\overline{C_1}$, $\overline{C_2}$	Laplace transform of concentrations of zone-1 and zone-2, respectively (mg/L).
S_i	Adsorbed concentrations for two zones (i=1, 2), (mg/L).
k_i	Empirical distribution coefficients for two zones, (i=1, 2).
ρ_i	Dry bulk density of soil for two zones (i=1, 2), (kg/m^3).
x	Flow direction, (m).
$\omega_{i,j}$	Constant values related to transport properties and Laplace variable s, (i=1, 2; j=3, 4).
A, B, E, F	Undetermined coefficients.
erfc	Complementary error function.

TABLE OF CONTENTS

Page

LIST OF FIGURES

Page

LIST OF TABLES

Page

1. INTRODUCTION

Groundwater is a very important natural resource that accounts for 30% of the total freshwater resources (Herschy and Fairbridge, 1998). The development of society and economy drives the rapid increase in the relative demand for groundwater supplies. In 2010, about 22.5% of total freshwater withdrawals in the United States came from groundwater sources, which has been widely used in public supply, industrial, and irrigation (Maupin et al., 2014).

There are various hazardous chemical substances and wastes in the groundwater environment, such as metals, radioactive elements, pesticides and herbicides, organic chemicals, petroleum products, pharmaceutical and health-care products, and microorganisms, whose damage to human health and environment is facilitated by their mobility in aquifers and, in some cases, solubility in water (Mulligan and Gibbs, 2001). Soil and groundwater pollution are common in the United States and many other countries as well. There were more than 1200 sites with contaminated soils waiting for treatment on the National Priority List in USA alone in 1996 and the list is still expanding (Hazardous Waste Consultant, 1996). Understanding solute transport in the subsurface is very important to evaluate and design natural and engineering containment barrier systems for containment and waste disposal, and remediate existing contaminated aquifer and soils (Sharma and Reddy, 2004).

The principal processes that affect the subsurface solute transport are believed to be advection, dispersion, sorption, chemical and biological decay, and other chemical

reactions (Freeze and Cherry, 1989; McCarty et al., 1980; Roberts et al., 1982). Advection is defined by the translation of the solute field by the bulk mass of flowing fluid. The concept of dispersion has been demonstrated by Taylor (1953) and subsequently discussed extensively by many others (Bear, 1972; Freeze and Cherry, 1979; Domenico and Schwartz, 1998). It is composed of both molecular and mechanical dispersion. Mechanical dispersion causes solute to mix by the velocity variations. Transverse dispersion causes spreading of the particles in directions perpendicular to the bulk flow. Diffusion describes the spread of solute through random motion in the direction of the concentration gradient (Freeze and Cherry, 1979). Sorption is the process of aqueous phase concentration decrease without changing the total mass through chemical reaction or microbiological interaction (Mackay et al., 1986). Based on these theories, one-dimensional advective-dispersive transport problem in homogeneous porous media with different boundary conditions has been solved by many investigators (van Genuchten and Alves, 1982; Sudicky and McLaren, 1992; Liu et al., 2000).

In practical contaminant transport problems, however, it is almost impossible to meet the simple situation with only one homogenous media. Usually, the porous media is heterogeneous and may include various zones which vary in their transport properties. Stochastic approaches have been used extensively for investigating subsurface transport in heterogeneous systems over many decades if one can quantify the statistical structure of the heterogeneous system (Gelhar, 1993; Zhang, 2002; Yeh et al., 2015), which is not always feasible in real-world applications. Therefore, deterministic approaches are still commonly used for understanding the subsurface transport. The available deterministic

approaches for subsurface transport include advection-dispersion equation (ADE) (Bear, 1972; Ervin and Roop, 2006), single-rate mobile and immobile theory (MIM) (van Genuchten and Wierenga, 1976; Rao et al., 1980), multi-rate mobile and immobile theory (MRMIM) (Haggerty and Gorelick, 1995; Silva et al., 2009), fractional advection-dispersion equation (FADE) (Benson et al., 2000), and continuous time random walk (CTRW) (Berkowitz et al., 2006; Benson et al., 2009). ADE is the simplest one built on the basis of Fick's law to describe the transport of solutes in saturated porous media by Bear (1972), and is still broadly used, particularly in solving practical engineering problems related to groundwater remediation. It could help assess the suitability of boundary conditions (Wehner and Wilhelm, 1956) and could also be used in the study of heat transport in geothermal reservoirs (Ortan et al., 2009; Molina-Giraldo et al, 2011), energy and mass transfer =(Pérez Guerrero et al., 2012) and gas fluxes measurements (Liu and Si, 2008).

Applying any of the above mentioned deterministic approaches (including ADE) for contaminant transport in heterogeneous media is challenging, as one has to face a few difficult issues such as scale-dependent dispersivity and various physical, geochemical, and biogeochemical processes. Fortunately, for some special cases, the media may be composed of several homogeneous zones and the transport properties for those zones could be well defined (Leij and van Genuchten, 1995). This kind of media is commonly found in stratified soils (Selim et al., 1977; Jacobson et al., 1992), landfill clay (Rowe et al., 1993), and aquifers and aquitards (Freeze and Cherry, 1979). Furthermore, contaminant transport in a two-zone system with quite different transport properties is

often observed in subsurface engineering problems. For example, in-situ capping of contaminated sediments (Lampert and Reible, 2009), and an underlying zone in waste disposal fields (Rowe et al., 2004) are two of the examples of transport in a two-zone media.

In this situation, contaminant transport in a two-zone or multi-zone system has been modeled by many investigators through numerical methods. Huyakorn et al. (1986) developed a finite-element formulation for contaminant dispersion in multi-zone systems. Leo and Booker (1999) used the boundary element method to analyze solute transport in heterogeneous media. Foose et al. (2002) employed one- and three-dimensional numerical models to simulate contaminant transport in the geomembrane component of composite liners. Although the transport problem could be solved by numerical models, analytical treatment is more commonly used, since it is straightforward to apply and is free from the numerical problems such as numerical dispersion and artificially oscillation issues that are sometime difficult to handle in the numerical simulations (Zheng and Bennett, 1995). In addition, it offers a screening tool which can be very important for decision making before an expensive groundwater remediation plan is implemented, and such a solution is useful for analyzing different and often correlated factors influencing the transport. Furthermore, it can be used as a benchmark to test any numerical solutions (Park and Zhan, 2001). Based on this theory, a number of mathematical models and associated analytical solutions in a two-zone or multi-zone system have been published over the past several decades (Al-Niami and Rushton, 1979; Leij et al., 1991; Liu et al., 1998).

There are two kinds of multi-zone media problems. In one of them, the flow direction is paralleled to the multi-zone interface. Al-Niami and Rushton (1979) investigated a two-zone system with the flow direction is paralleled to the interface. They defined each zone separately with the consideration of lateral diffusion between interactive interfaces, and used integral transform combined with Laplace transformation to obtain the analytical solutions when longitudinal dispersion coefficients of the two zones are the same. This kind of problem has received much less attention than the problem in which the flow direction is perpendicular to the multi-zone interface.

Shamir and Harleman (1967) studied such a two-zone system with the flow direction perpendicular to the multi-zone interface. He treated the first zone as an initial condition and used the analytical solution of a semi-finite medium to calculate the concentration in the first zone, and then used the ending concentration of the first zone as an input boundary condition to calculate the concentration for the second zone. This method is physically questionable in several aspects. Firstly, separating an integrated two-zone system into two different boundary value problem violated the mass conservation law in general. Secondly, the assumption of zero concentration gradient condition at the interface between two zones is also untrue (Leij et al., 1991). Li and Cleall (2011) changed the boundary condition of interfaces to remedy the problem of Shamir and Harleman (1967), which considered both solute flux continuity and concentration gradient continuity at the interface of the two zones. The solutions have been derived under five different situations in Li and Cleall (2011).

Liu et al. (1998) obtained more general solutions through a generalized integral transform (GITT) method for solving ADE in an *M*-zone media of steady-state flow with inlet boundary conditions, where *M* could be any positive integer number theoretically. The solution is expressed in a matrix form and it is flexible with the inlet condition. However, this method is complex and requires the coefficient to be determined in the fully filled matrix, and it also requires a large number of numerical calculations as an analytical solution in principle.

Shen et al. (2015) also worked on the same problem for a multi-zone system as Liu et al. (1998). Shen et al. (2015) used the variables separation method to derive the analytical solution and obtained a solution included hyperbolic eigenfunctions and trigonometric eigenfunctions. Shen et al. (2015) thought that this method was better than GITT since its solution converged faster and required a simpler coefficient determination than GITT. Though this method improved on the previous method, it is still difficult to calculate eigenvalues with high Peclet number (over 100).

Despite the fact that many studies have been performed for the solution of contaminate transport in multi-zone systems, the subsurface solute transport in heterogeneous geological systems is still complex and difficult to simulate in dealing with practical engineering problems. Therefore, scientists and engineers are trying to use the averaging approach (or homogenization) to study the flow simulation and make engineering decisions, which could scale up the fine scale heterogeneous zones to the larger scales.

Liu et al. (1998) drew the breakthrough curves (BTCs) of a five-zone case and compared it to a one-zone case with averaged parameter values such as retardation factor, dispersion coefficient, velocity, and porosity. The BTCs of the five-zone and one-zone did not fit with each other well, which showed that the simple average of transport property is not always appropriate for the homogenization. Gelhar and Axness (1983) developed a perturbation approach to determinate effective permeability in porous media with heterogeneous permeability fields. They used an exponential covariance function to describe random logarithmic permeability field, but their results were only valid to small perturbation of the randomness of the logarithmic permeability field.

The common method for homogenization is the representative elementary volume (REV) method, which calculates equivalent parameters and uses them as the effective parameters for the whole region. Durlofsky (1991) established a triangle-based finite-element numerical approach to calculate the homogenization of permeability. This homogenization process is based on a two-scale formulation and is limited to large scale flow through heterogeneous media and the effective permeability is dependent on the scale of heterogeneity. Amaziane at al. (1991) developed a finite-element method based on asymptotic expansions and H-convergence to calculate the homogenized coefficients for two-phase flow in heterogeneous porous media. Their theory did not consider boundary layers which were assumed to have no effect on the results of the homogenized results. Held et al. (2005) investigated a two-dimensional Henry problem in coastal aquifer through theoretical and numerical method to upscale the density-dependent flow. Based

on the homogenization theory, the effective transport properties had been found in the statistically isotropic and anisotropic heterogeneous permeability zones.

A common feature in above upscaling studies is that spatial correlation of the heterogeneous porous media should be known a priori. When conducting the homogenization of heterogeneity zones, length scales of heterogeneous porous media always need to be considered. Scientists and engineers found that longitudinal dispersivity increasing with mean travel distance in many field tracer (Peaudecerf and Sauty, 1978; Freyberg, 1986). Gelhar et al. (1992) descripted the observation of "scale-dependent dispersion" that the dispersivity variation depended on the changing degrees of aquifer heterogeneity. But they found that the scale dependence of dispersivity was less clear when the longitudinal dispersivity data classified by reliability. Neuman et al. (1987) developed an asymptotic dispersivity tensor for field-scale dispersivity in three-dimensional statistically anisotropic media. They found that the principal dispersivities increased with Peclet numbers when the Peclet numbers were small. Neuman (1990) provided an interpretation for the scale-dependent issue with universal scaling law for hydraulic conductivity and this study was based on the randomness assumption. Rajaram and Gelhar (1993) described an analytical approach with plume displacement at the plume scale to investigate the observation of dispersivity changed with length scale. The results showed that the longitudinal dispersivity growth rate was relative to the transverse of the plume. Therefore, the scale-dependent issue is very important to the study of heterogeneous system and the calculation of equivalent parameters.

From above studies, one can see that there is little research related to the influence of the order of heterogeneity (or the reversal of groundwater flow direction) on the solute transport and the homogenization of the parameters. The objectives of this thesis are to answer the following key scientific questions: 1) For a two-zone heterogeneous system, when the positions of the two zones reverse and while other conditions remain the same, will the BTCs remain the same or not? 2) Is that possible to simplify a two-zone heterogeneous system into an averaged homogeneous system for transport? 3) If the answer to above question 2) is true, then what is the relationship between the homogenized transport properties and the transport properties of those two-zones? And can one see the scale-dependency of the homogenized transport properties such as dispersivity? This research will help describe the order of heterogeneity influence on migration of chemical solute in aquifers. Such a two-zone investigation can serve as a base for investigating a heterogeneous system with more than two zones.

2. PROBLEM STATEMENT

2.1 Conceptual Model

The research model has two individual homogeneous zones (namely zone-1 and zone-2) with different transport properties, as illustrated in Fig.1. The flux flows in the positive *x*-axis direction, which is perpendicular with the interface of zone-1 and zone-2, and is characterized by the Darcy velocity *q*. The inlet and outlet boundaries are defined at *x*=0 and *x*=*L*. The transport process also includes a first-order reaction and a linear sorption scheme, in addition to advection and dispersion. Each zone has its own retardation factor (R_i), constant dispersion coefficient (D_i), porosity (θ_i), and reaction rate (λ_i). The subscript *i* represents the zone with *i*=1 corresponding to zone-1 and *i*=2 to zone-2. The length of zone-1 is L_1 and the total length of two zones is *L*.

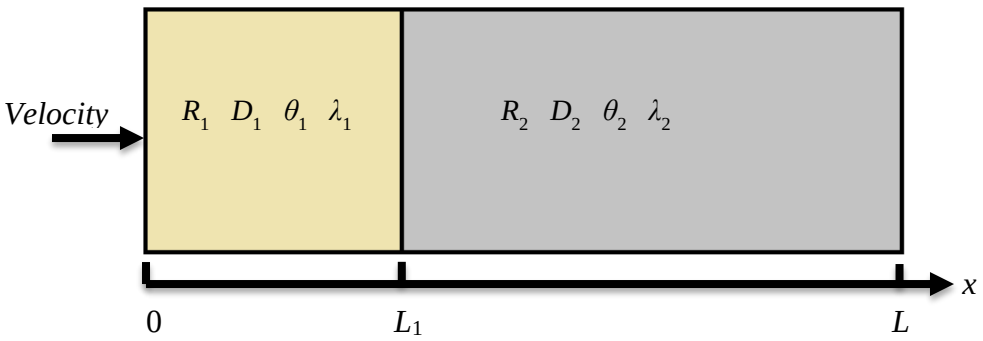

Figure 1. Schematic of contaminant transport in two homogenous zones with different transport properties.

Governing transport equations

ADE is often used to describe the contaminant transport in homogeneous porous media, and is also the basis for further advanced theories for studying contaminant transport in heterogeneous media. One-dimensional ADE derived by Bear (1972) without decay and sink/source terms is:

$$R\frac{\partial C}{\partial t}=\frac{\partial}{\partial x}\left(D\frac{\partial C}{\partial x}\right)-v\frac{\partial C}{\partial x}, \tag{2-1}$$

where C is the concentration of the adsorbate in solution [M·L^{-3}], v=q/θ is the average pore velocity [L·T^{-1}], q is Darcy's velocity [L·T^{-1}], θ is porosity, t is time [T], x is the longitudinal dimension along the direction of flow [L], D is the dispersion coefficient [L^2·T^{-1}], R is a retardation factor associated with linear sorption [dimensionless].

In this thesis, a first-order decay has been considered. Because two zones are homogeneous individually, θ and q are constant in time and space. Assume that the adsorbed concentrations (S_i) which is defined as the ratio of the sorbed mass over the mass of the media, can be related to solution concentrations (C_i) by linear and reversible isotherms of the form:

$$S_i=k_iC_i \qquad (i=1,2), \tag{2-2}$$

where k_i are empirical distribution coefficients [M·L^{-3}].

Then the following governing transport equations will be used:

$$R_1\frac{\partial C_1}{\partial t}=D_1\frac{\partial^2 C_1}{\partial x^2}-v_1\frac{\partial C_1}{\partial x}-\lambda_1R_1C_1, \tag{2-3}$$

$$R_2\frac{\partial C_2}{\partial t}=D_2\frac{\partial^2 C_2}{\partial x^2}-v_2\frac{\partial C_2}{\partial x}-\lambda_2R_2C_2, \tag{2-4}$$

where the subscripts 1 and 2 represent the terms for the first and second zones, respectively hereinafter, C_1 and C_2 are the concentrations of the adsorbate in solution [M·L^{-3}], λ_1 and λ_2 are reaction rates [1/T], $v_1$and v_2 are the average pore velocities [L·T^{-1}] given by

$$v_1 = q / \theta_1 \ , \quad v_2 = q / \theta_2 , \tag{2-5}$$

where θ_1 and θ_2 are the porosities.

D_1 and D_2 are the dispersion coefficients [L^2·T^{-1}] given by

$$D_1 = v_1 \times \alpha_1 , \quad D_2 = v_2 \times \alpha_2 \ , \tag{2-6}$$

after negating molecular diffusion, α_1 and α_2 are the longitudinal dispersivity values [L], $R_1$and R_2 are retardation factors associated with linear sorption given by

$$R_i = 1 + \frac{\rho_i k_i}{\theta_i} \ , \tag{2-7}$$

where ρ_i are dry bulk density of soil (i=1, 2), k_i are empirical distribution coefficients [M·L^{-3}].

Initial and boundary conditions

In this study, the analytical solutions are applicable to finite systems$(0 \le x \le L)$. Using the Danckwerts boundary condition to force discontinuities in concentration and its gradient at the column exit, and avoid the situation that solute concentration in the column is beyond the maximum or minimum concentration (Danckwerts, 1953)

$$\left. \frac{\partial C_2}{\partial x} \right|_{x=L} = 0 . \tag{2-8}$$

The system is free of solutes at the beginning, thus the initial condition is

$$C_1\left(x,t=0\right)=0\,,\ C_2\left(x,t=0\right)=0 \tag{2-9}$$

and the input boundary condition at $x = 0$ is described by the third-type condition, which ensures mass conservation at the x=0 (van Genuchten and Parker, 1984),

$$\left(v_1C_1 - D_1\frac{\partial C_1}{\partial x}\right)\Bigg|_{x=0} = v_1C_0\ . \tag{2-10}$$

Continuities of concentration and mass flux across the interfacial of two zones lead to

$$C_1\big|_{x=L_1} = C_2\big|_{x=L_1}\ , \tag{2-11}$$

$$-\theta_1D_1\frac{\partial C_1}{\partial x}\bigg|_{x=L_1} = -\theta_2D_2\frac{\partial C_2}{\partial x}\bigg|_{x=L_1}\ . \tag{2-12}$$

2.2 Main Tasks

I will follow the following steps to investigate the problem. Firstly, I will solve ADE in a two-zone media with the first-order reaction and the linear sorption analytically in Laplace domain, and I will use the de Hoog algorithm for inverse Laplace transform to obtain the solution in real-time domain. The result will be verified by a closed-form analytical solution for a special homogeneous case. This part will be discussed in Section 3.

Secondly, I will study the influence of the order of heterogeneity on solute transport. To do this I will calculate the concentration distribution in a two-zone media with different transport properties, and use this to plot BTCs at the end of the two-zone media. After this, I will switch the positions of two zones (reverse the order of

heterogeneity) and repeat the above steps to obtain the concentration distribution and BTCs again. Then I will compare BTCs to analyze the influence of order of heterogeneity on concentration distribution, which will be discussed in Section 4.1.

Thirdly, I will vary the values of certain parameters to discover how contrasting parameter values between two zones will affect the results when the order of heterogeneity reverses. Several cases will be set up, eight of them will only have a single parameter varied between zone-1 and zone-2, and the remaining cases have multiple parameters varied between zone-1 and zone-2. I will compare the results and try to find out which parameter(s) will affect results the most. This part will be explained in Section 4.2.

Fourthly, I will use a curve-fitting function written in MATLAB script files to determine the optimal parameter values after the homogenization of the two-zone heterogeneous media. I will try to see whether the order of heterogeneity will impact the result or not. This part will be discussed in Section 4.3.

Finally, I will discuss the scale-dependence of dispersivity of the homogenized media, which will be illustrated in Section 4.4.

3. METHODOLOGY

3.1 Analytical Solutions for Transport in a Two-zone System

In this section, the analytical solutions for the advective-dispersive transport process including first-order reaction and linear sorption in a two-zone porous media will be found through following steps.

The total length L is used as the characteristic length scale. The dimensionless variables are defined by this scale combined with retardation factor (R_i), dispersion coefficient (D_i), porosity (θ_i), reaction rate (λ_i), and initial constant source concentration (C_0):

$$C_{1D} = \frac{C_1}{C_0}; \quad C_{2D} = \frac{C_2}{C_0}; \quad t_D = \frac{D_1}{L^2} t; \quad x_D = \frac{x}{L}, \tag{3-1}$$

$$P_{e1} = \frac{v_1 L}{D_1}, \; P_{e2} = \frac{v_2 L}{D_2}, \tag{3-2}$$

$$\beta = \frac{D_2}{D_1}; \quad \lambda_{1D} = \frac{\lambda_1 L^2}{D_1}; \quad \lambda_{2D} = \frac{\lambda_2 L^2}{D_2}; \quad \mathrm{L}_{1D} = \frac{L_1}{L}; \quad \gamma = \frac{\theta_2}{\theta_1} = \frac{v_1}{v_2}. \tag{3-3}$$

The dimensionless governing equations are normalized to:

$$R_1 \frac{\partial C_{1D}}{\partial t_D} = \frac{\partial^2 C_{1D}}{\partial x_D{}^2} - P_{e1} \frac{\partial C_{1D}}{\partial x_D} - \lambda_{1D} R_1 C_{1D}, \tag{3-4}$$

$$R_2 \frac{\partial C_{2D}}{\partial t_D} = \beta \frac{\partial^2 C_{2D}}{\partial x_D{}^2} - \beta P_{e2} \frac{\partial C_{2D}}{\partial x_D} - \beta \lambda_{2D} R_2 C_{2D}, \tag{3-5}$$

and the dimensionless initial and boundary conditions are:

$$\left(C_{1D} - \frac{1}{P_{e1}} \frac{\partial C_{1D}}{\partial x_D} \right) \Bigg|_{x_D=0} = 1, \tag{3-6}$$

$$C_{1D}\left(t_D = 0\right) = 0 \ , \ C_{2D}\left(t_D = 0\right) = 0 \tag{3-7}$$

$$C_{1D}\big|_{x_D=L_{1D}} = C_{2D}\big|_{x_D=L_{1D}}, \tag{3-8}$$

$$\frac{\partial C_{1D}}{\partial x_D}\Bigg|_{x_D=L_{1D}} = \gamma\beta \frac{\partial C_{2D}}{\partial x_D}\Bigg|_{x_D=L_{1D}} , \tag{3-9}$$

$$\frac{\partial C_{2D}}{\partial x_D}\Bigg|_{x_D=1} = 0 . \tag{3-10}$$

There are many different methods to obtain analytical solutions of advection-dispersion transport equation in multi-zone media, such as Laplace transform method, integral transform method and the method comprised the Laplace transformation and binomial theorem. In this thesis, Laplace transformation techniques will be used to derive the equation. Laplace transformation method could provide an alternative functional description without solving eigenfunctions and simplify the process of converting the governing equations based on the initial and boundary conditions (Korn and Korn, 1968).

Taking Laplace transform and denoting $\overline{C_{1D}} = L[C_{1D}]$, $\overline{C_{2D}} = L[C_{2D}]$, where $L[\ ]$ is the Laplace operator, and overbar implies the terms in Laplace domain, Eq. (2-3) and (2-4) could transform to:

$$sR_{1D}\overline{C_{1D}} = \frac{d^2\overline{C_{1D}}}{dx_D^{\ 2}} - P_{e1}\frac{d\overline{C_{1D}}}{dx_D} - \lambda_{1D}R_1\overline{C_{1D}} , \tag{3-11}$$

$$\mathrm{s}R_{2D}\overline{C_{2D}} = \beta\frac{d^2\overline{C_{2D}}}{dx_D^{\ 2}} - \beta P_{e2}\frac{d\overline{C_{2D}}}{dx_D} - \beta\lambda_{2D}R_{2D}\overline{C_{2D}} , \tag{3-12}$$

where *s* is Laplace variable in respect to the dimensionless time.

The associated boundary conditions in Laplace domain become:

$$\left(\overline{C_{1D}} - \frac{1}{P_{e1}}\frac{d\overline{C_{1D}}}{dx_D}\right)\Bigg|_{x_D=0} = \frac{1}{s} \ , \tag{3-13}$$

$$\overline{C_{1D}}\Big|_{x_D=L_{1D}} = \overline{C_{2D}}\Big|_{x_D=L_{1D}} \ , \tag{3-14}$$

$$\frac{d\overline{C_{1D}}}{dx_D}\Bigg|_{x_D=L_{1D}} = \gamma\beta\frac{d\overline{C_{2D}}}{dx_D}\Bigg|_{x_D=L_{1D}} \ , \tag{3-15}$$

$$\frac{d\overline{C_{2D}}}{dx_D}\Bigg|_{x_D=1} = 0 \ . \tag{3-16}$$

Set up $\overline{C_{1D}} \sim e^{-\omega_i x}$ and $\overline{C_{2D}} \sim e^{-\omega_j x}$, where $\omega_i (i = 1, 2)$and $\omega_j (j = 3, 4)$ are the constant values related to transport properties and Laplace variable *s*. Then the Eq. (3-11) and Eq. (3-12) come to:

$$sR_{1D} = \omega_i^2 + P_{e1}\omega_i - \lambda_{1D}R_{1D} \ , \tag{3-17}$$

$$sR_{2D} = \beta\omega_j^2 + \beta P_{e2}\omega_j - \beta\lambda_{2D}R_{2D} \ . \tag{3-18}$$

Solving the quadratic equations, the results come out:

$$\omega_1 = \frac{-P_{e1} + \sqrt{P_{e1}^2 + 4\left(\lambda_{1D} + s\right)R_{1D}}}{2} \quad \omega_2 = \frac{-P_{e1} - \sqrt{P_{e1}^2 + 4\left(\lambda_{1D} + s\right)R_{1D}}}{2} \ , \tag{3-19}$$

$$\omega_3 = \frac{-P_{e2} + \sqrt{P_{e2}^2 + 4\left(\lambda_{2D} + \frac{s}{\beta}\right)R_{2D}}}{2} \quad \omega_4 = \frac{-P_{e2} - \sqrt{P_{e2}^2 + 4\left(\lambda_{2D} + \frac{s}{\beta}\right)R_{2D}}}{2} \tag{3-20}$$

According to the results of Eq. (3-19) and (3-20), one can set up:

$$\overline{C_{1D}} = Ae^{-\omega_1 x} + Be^{-\omega_2 x} \ , \tag{3-21}$$

$$\overline{C_{2D}} = Ee^{-\omega_3 x} + Fe^{-\omega_4 x} \ , \tag{3-22}$$

where *A*, *B*, *E*, *F* are undetermined constant coefficients.

Substituting Eqs. (3-21) and (3-22) into the boundary conditions of Eqs. (3-13), (3-14), (3-15), and (3-16), one has:

$$A + B - \frac{1}{P_{e1}}\left(-A\omega_1 - B\omega_2\right) = \frac{1}{s} \ , \tag{3-23}$$

$$Ae^{-\omega_1 L_1} + Be^{-\omega_2 L_1} = Ee^{-\omega_3 L_1} + Fe^{-\omega_4 L_1} \ , \tag{3-24}$$

$$-\omega_1 Ae^{-\omega_1 L_1} - \omega_2 Be^{-\omega_2 L_1} = -\gamma\beta\omega_3 Ee^{-\omega_3 L_1} - \gamma\beta\omega_4 Fe^{-\omega_4 L_1} \ , \tag{3-25}$$

$$-\omega_3 Ee^{-\omega_3} - \omega_4 Fe^{-\omega_4} = 0 \ . \tag{3-26}$$

Solving above equation group of (3-23) to (3-26), one can obtain *A*, *B*, *E*, and *F*, which can be substituted into Eqs. (3-21) and (3-22) to yield:

$$\begin{aligned}\overline{C_{1D}} = \frac{P_{e1}}{s}\Bigg(&-\frac{1}{\omega_2} - \frac{\omega_1}{\omega_2} \times \frac{\omega_1\left(\omega_3\alpha^{L_1} - \omega_4\alpha\right) + \gamma\beta\omega_4\omega_3\left(\alpha - \alpha^{L_1}\right)}{\gamma\beta\omega_3\omega_4\left(\alpha - \alpha^{L_1}\right)\left(\omega_2\delta^{L_1} - \omega_1\right) + \left(\omega_3\alpha^{L_1} - \omega_4\alpha\right)\left(-\omega_1^{\ 2} + \omega_2^{\ 2}\delta^{L_1}\right)}\Bigg) e^{-\omega_1 x} \\ &+ \frac{P_{e1}}{s} \frac{\omega_1\left(\omega_3\alpha^{L_1} - \omega_4\alpha\right) + \gamma\beta\omega_4\omega_3\left(\alpha - \alpha^{L_1}\right)}{\gamma\beta\omega_3\omega_4\left(\alpha - \alpha^{L_1}\right)\left(\omega_2\delta^{L_1} - \omega_1\right) + \left(\omega_3\alpha^{L_1} - \omega_4\alpha\right)\left(-\omega_1^{\ 2} + \omega_2^{\ 2}\delta^{L_1}\right)} e^{-\omega_2 x}\end{aligned} \ , \tag{3-27}$$

$$\overline{C_{2D}} = \left(\begin{array}{c} -\frac{P_{e1}\omega_3 e^{(\omega_3 - \omega_1)L_1}}{s\left(\omega_2\omega_3\alpha^{L_1} - \omega_2\omega_4\alpha\right)} + \frac{e^{(\omega_3 - \omega_2)L_1} - \frac{\omega_1}{\omega_2} e^{(\omega_3 - \omega_1)L_1}}{\alpha^{L_1} - \frac{\omega_4}{\omega_3}\alpha} \times \\ \left(\frac{P_{e1}}{s} \frac{\omega_1\left(\omega_3\alpha^{L_1} - \omega_4\alpha\right) + \gamma\beta\omega_4\omega_3\left(\alpha - \alpha^{L_1}\right)}{\gamma\beta\omega_3\omega_4\left(\alpha - \alpha^{L_1}\right)\left(\omega_2\delta^{L_1} - \omega_1\right) + \left(\omega_3\alpha^{L_1} - \omega_4\alpha\right)\left(-\omega_1^{\ 2} + \omega_2^{\ 2}\delta^{L_1}\right)} \right) \end{array} \right) \times \left(-\frac{\omega_4 \times \alpha}{\omega_3} e^{-\omega_3 x} + e^{-\omega_4 x} \right) , \tag{3-28}$$

where $\alpha = e^{\omega_3 - \omega_4}$, $\delta = e^{\omega_1 - \omega_2}$, and the detailed derivation procedures are shown in Appendix A.

Laplace inverse transformation

It appears to be very difficult to analytically invert the above solutions in Laplace domain into their real-time solutions. As a result, the inverse Laplace transform has to be conducted numerically (Barry and Parler, 1987; Leij et al., 1991). Fortunately, there are several widely used methods to do the inverse Laplace transform, such as the Stehfest, the de Hoog, the Talbot, the Simon, the Weeks, the Honig-Hirdes, and the Zakian methods, as discussed in details by Wang and Zhan (2015). From the study of Wang and Zhan (2015), the de Hoog, the Talbot and the Simon methods work well for radial dispersion problems, regardless of the advection-dominated or dispersion-dominated problems with numerical accuracy. Compared to other methods, the de Hoog algorithm would improve the accuracy of result by reducing errors through discretization and rounding, and accelerate the convergence of the series, which could be applied to the advection-dispersion problem of this study.

Boupha et al. (2004) have shown that the de Hoog method is very robust in dealing with many transport problems. Using Laplace transform method and then applied the de Hoog algorithm to invert the Laplace domain solution has been employed to solve the advection-dispersion problems by many other investigators such as Hatfield and Stauffer (1993) and Hatfield et al. (1996), who obtained the accurate solutions of one-, two-, and three-dimensional solute transport problems through this method.

Based on the de Hoog method (Hollenbeck, 1998), I developed MATLAB script files listed in Appendix B to facilitate the computation of this thesis.

3.2 Verification of the Developed Semi-analytical Solution

The developed semi-analytical solution was compared to the analytical solution for some special cases of one-dimensional transport in a homogeneous media in this section. To do so, one let zone-1 and zone-2 have the same transport properties.

The analytical solution for a special case of one-dimensional transport in a semi-infinite homogeneous media with the first-kind boundary condition at x=0 m ignored decay and sorption has been reported in many previous investigations and is expressed as (Fetter, 1999):

$$\frac{C}{C_0}=\frac{1}{2}\left[erfc\left(\frac{x-vt}{2\sqrt{Dt}}\right)+\exp\left(\frac{vx}{D}\right)erfc\left(\frac{x+vt}{2\sqrt{Dt}}\right)\right], \tag{3-29}$$

where erfc is the complementary error function and defined by

$$erfc(z)=\frac{2}{\sqrt{\pi}}\int_z^{\infty}e^{-t^2}dt\ . \tag{3-30}$$

For the purpose of comparison, one can set up the test cases 1-3 without decay and sorption, which shows in table 1. The BTCs consisting of the relative concentration (C/C_0) and time at the end of column is shown in Fig. 2.

Table 1. The transport properties of tests 1-3.

Test No.	L (m)	θ_1	θ_2	α_1 (m)	α_2 (m)	R_1	R_2	λ_1 (1/d)	λ_2 (1/d)
1	100	0.1	0.1	1	1	1	1	0	0
2	80	0.2	0.2	2	2	1	1	0	0
3	80	0.3	0.3	2	2	1	1	0	0

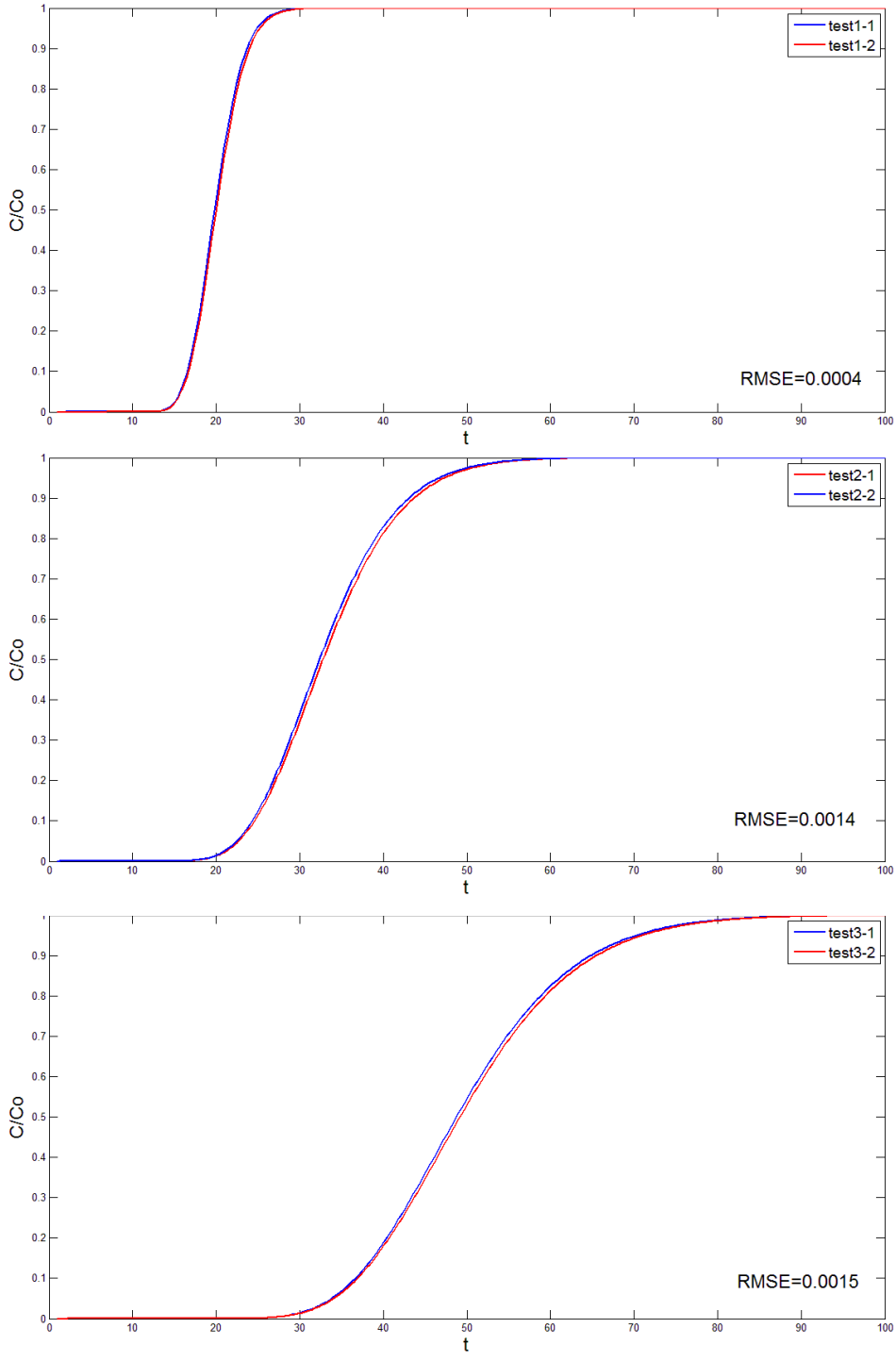

Figure 2. BTCs obtained with the semi-analytical solution of this study the Eq. (3-29) for a homogenous media at the end of column for tests 1-3. Dash 1 represents the semi-analytical solution of this study, and dash 2 represents Eq. (3-29).

The result shows that BTCs obtained with two methods fit with each other very well. The root-mean-square-error (RMSE) is small, which means the differences between two curves is negligibly small. From this comparison, the semi-analytical solution developed in this study appears to be correct and reliable.

4. CASE STUDY

4.1 Heterogeneity Structure Influence

To investigate the order of heterogeneity influence on the contaminant transport in a two-zone system, the following transport properties are used for the purpose of illustration: q =0.5m/day, θ_1 =0.3, θ_2 =0.2, α_1 =1m, α_2 =3m, L_1 =40m, L =100m, $R_1 = R_2$ =1.2, $\lambda_1 = \lambda_2$ =0.01day^{-1}, which given by $\lambda = \ln 2 / T_{1/2}$, $T_{1/2}$ is the half-life ofa reaction.

I will simulate two scenarios separately: in case 1-1, the flow direction is from zone-1 to zone-2. In case 1-2, the zone-1 and zone-2 switches their positions, and the other conditions remain the same for as case 1-1, which means the flow direction is from zone-2 to zone-1. Fig. 3 is the BTCs at L=100m for these two scenarios.

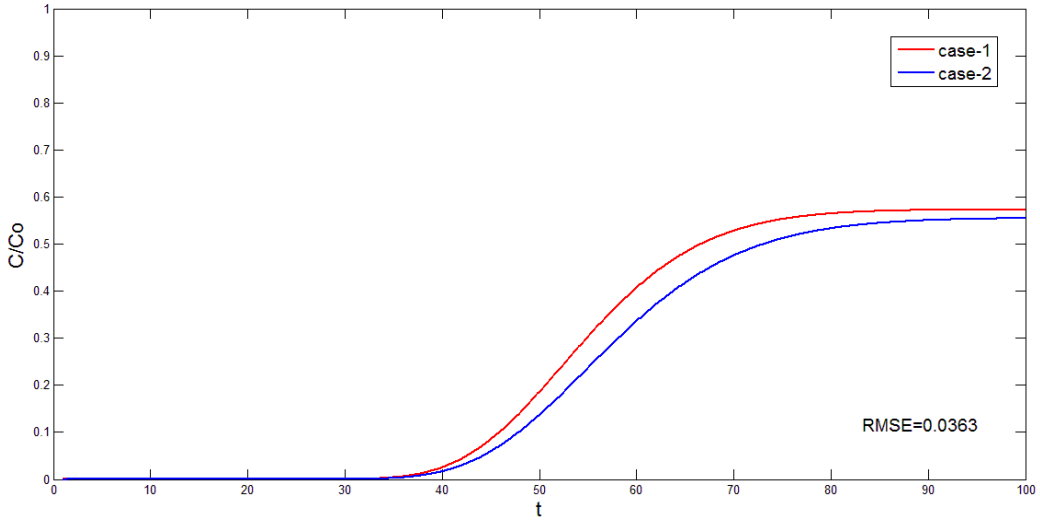

Figure 3. BTCs at L=100m for cases 1-1 and 1-2.

From Fig. 3, we can clearly see that the order of heterogeneity will affect the contaminant transport in a two-zone porous media. Notice that the computed concentrations are different for these two cases. The relative concentration reaches its asymptotic (steady-state) value faster in case 1-1than in case 1-2, and its asymptotic value is greater than that in case 1-2. The reason of this observation will explain in the section 4.2.

4.2 Influence of Transport Properties of Two-zones

This section is devoted to analyze how the difference of transport properties of zone-1 and zone-2 will impact on the contaminant transport when the order of heterogeneity reverses. To do so, one can change one or more parameter values for zone-1 and zone-2 but keep the rest parameter values of these two zones the same. The retardation factor (R_i), dispersivity (α_i), porosity (θ_i), reaction rate (λ_i), and the length of zone-1 (L_1) are the main transport properties which will affect the solute transport in the porous media. Table 2 shows the transport properties of cases 2-15.

Table 2. Transport properties of conceptual cases 2-15.

Case No.	L_1 (m)	θ_1	θ_2	α_1 (m)	α_2 (m)	R_1	R_2	λ_1 (1/d)	λ_2 (1/d)
2	50	**0.2**	**0.4**	1	1	1	1	0	0
3	50	**0.1**	**0.4**	1	1	1	1	0	0
4	50	0.3	0.3	**1**	**2**	1	1	0	0
5	50	0.3	0.3	**1**	**4**	1	1	0	0

Table 2. Continued.

Case No.	L_1 (m)	θ_1	θ_2	α_1 (m)	α_2 (m)	R_1	R_2	λ_1 (1/d)	λ_2 (1/d)
6	50	0.3	0.3	1	1	**2**	**4**	0	0
7	50	0.3	0.3	1	1	**2**	**8**	0	0
8	50	0.3	0.3	1	1	1	1	**0.01**	**0.02**
9	50	0.3	0.3	1	1	1	1	**0.01**	**0.04**
10	**50**	0.15	0.3	4	1	3	2	0	0
11	**40**	0.15	0.3	4	1	3	2	0	0
12	**10**	0.15	0.3	4	1	3	2	0	0
13	**50**	0.3	0.3	2	3	2	1.5	0.01	0.02
14	**40**	0.3	0.3	2	3	2	1.5	0.01	0.02
15	**10**	0.3	0.3	2	3	2	1.5	0.01	0.02

All cases have the same Darcy velocity q=0.5m/day and the total length of two zones L is 100m. For cases 2-9, there is only one transport property different between two zones, and zone-1 always has a lower parameter value than zone-2. For cases 10-15, there are several transport properties different between two zones. The transport properties between cases 10-12 are the same except lengths of zone-1 and zone-2. So as the cases 13-15.

Porosity influence

In cases 2 and 3, the porosities are different in two zones and other parameters are the same. In case 2, the ratio of porosity in zone-2 to zone-1 is 2, and in case 3 such a porosity ratio is 4. Fig. 4 shows the BTCs for cases 2 and 3 and their heterogeneity reversed situation at L=80m and L=100m.

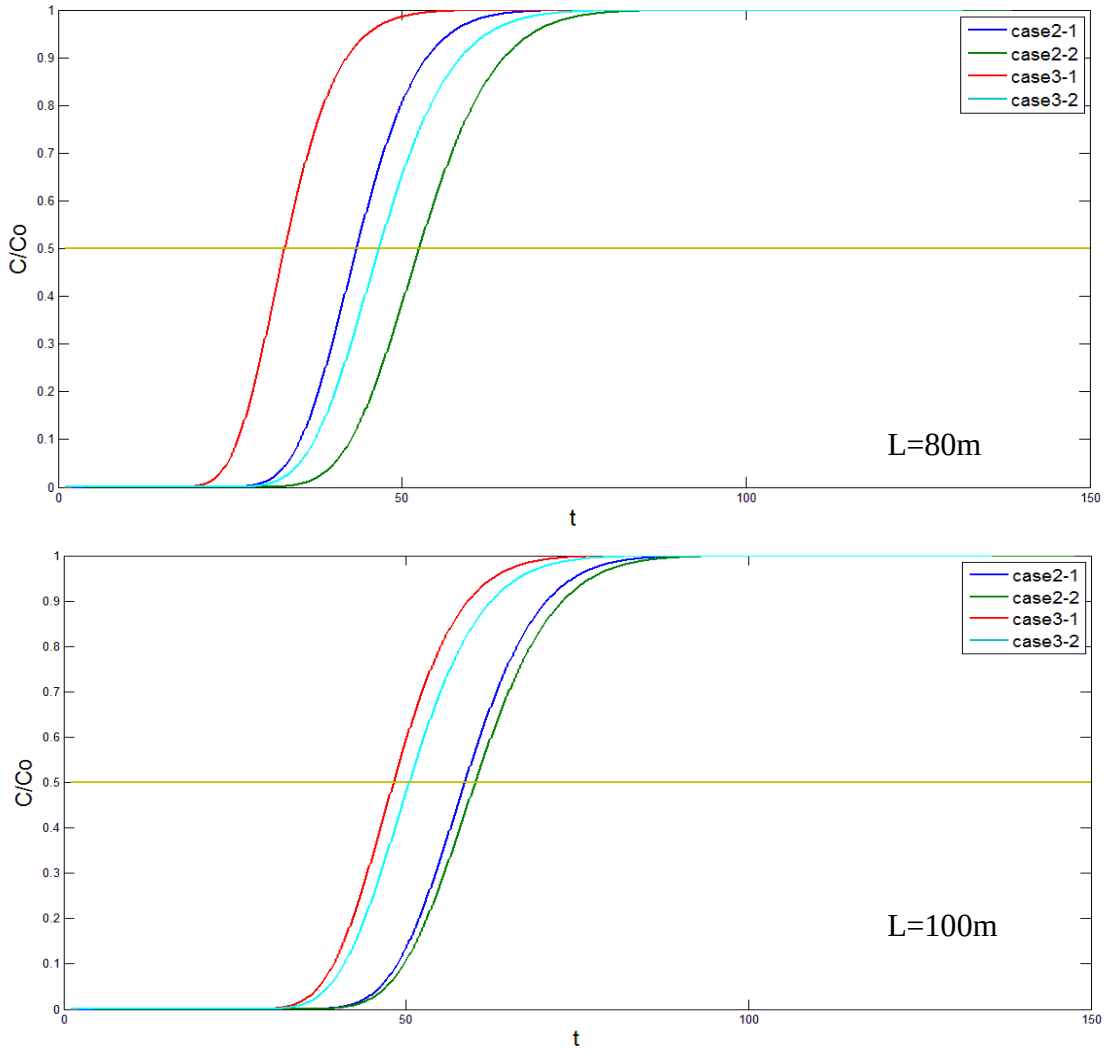

Figure 4. BTCs for cases 2-3 at L=80m and L=100m, where dash 1means flow direction is from zone-1 to zone-2, and dash 2 means flow direction is from zone-2 to zone-1.

Table 3. Transport situations for cases 2-3 (porosity difference).

Case No.	Flow direction	$\theta_{upstream}/\theta_{downstream}$	T at the midpoint (L=80m)	Midpoint width (L=80m)	T at the midpoint (L=100m)	Midpoint width (L=100m)
2-1	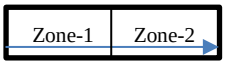	0.5	43.5	9.1	58.7	1.5
2-2	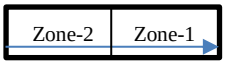	2	52.6		60.2	
3-1	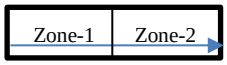	0.25	33.1	13.6	48.2	2.3
3-2	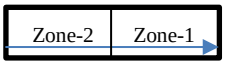	4	46.7		50.5	

The BTCs and widths between midpoints of both cases show that when the difference of porosities between two zones increases, the width of midpoints of BTCs increases as well, which means the influence of solute transport increases when the order of heterogeneity reverses. When reversing the two zones' positions, the relative concentration takes less time to reach its asymptotic value with the flux flows from the lower porosity zone to the higher porosity zone. When the ratio of upstream porosity to downstream porosity is greater than 1, a higher ratio shows a higher relative concentration at a given time. This can be explained as follows. Due to the relationship of $v=q/n$, a lower porosity means a higher velocity. In case 2-1, thus the solute will reach the interface earlier than that in case 2-2, and zone-2 will have a higher concentration than that in case 2-2 at the same given time. When the time is long enough, the relative concentration will reach 1.0 without sorption and reaction.

Dispersivity influence

In cases 4 and 5, the dispersivity is the only different parameter in two zones. In case 4, the ratio of dispersivity in zone-2 to zone-1 is 2, and in case 5 such a ratio is 4. Fig.5 shows the BTCs for cases 4 and 5 and their heterogeneity reversed situation at L=80m and L=100m.

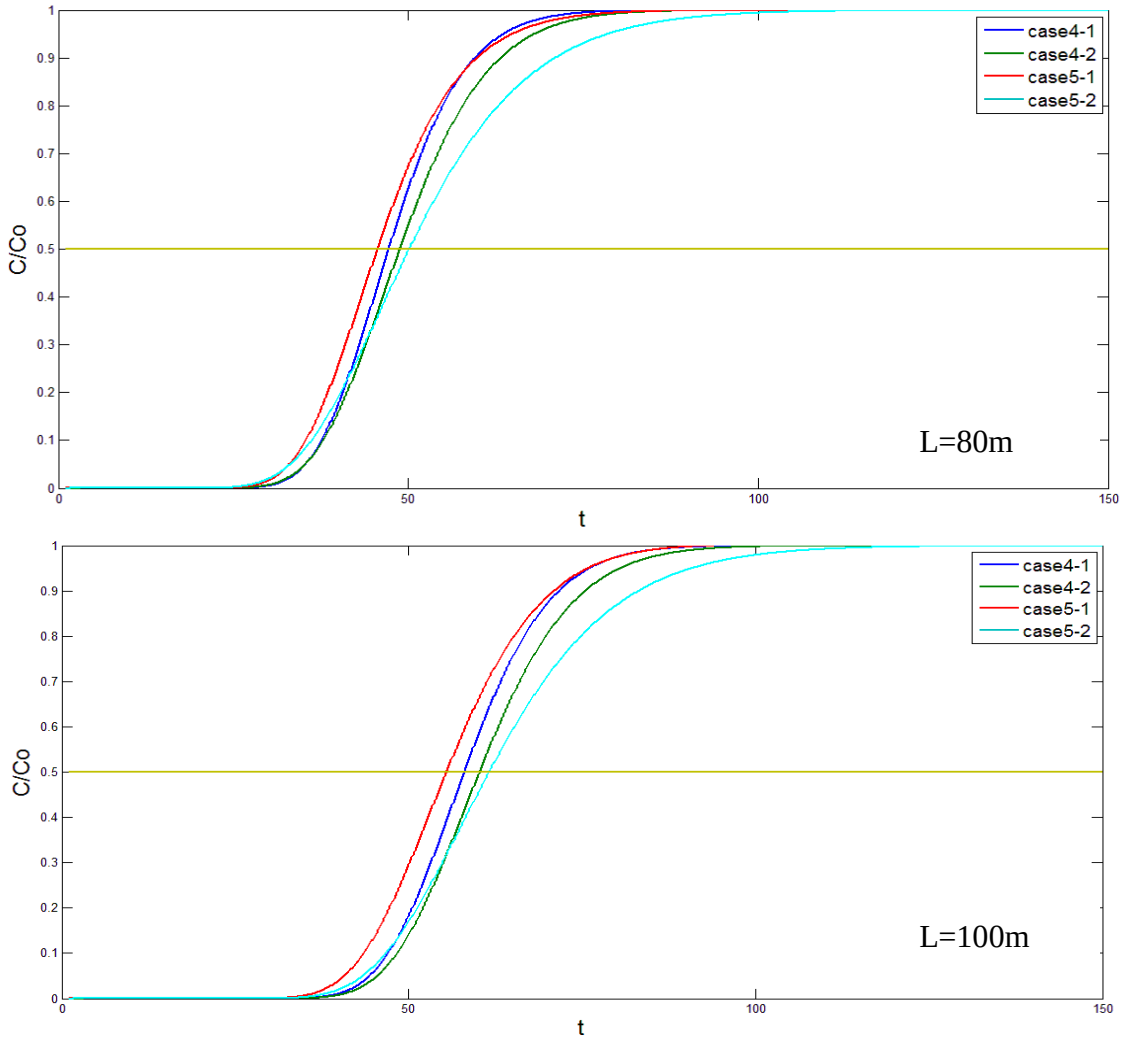

Figure 5. BTCs for cases 4-5 at L=80m and L=100m, where dash 1means flow direction is from zone-1 to zone-2, and dash 2 means flow direction is from zone-2 to zone-1.

Table 4. Transport situations for cases 4-5 (dispersivity difference).

Case No.	Flow direction	$\alpha_{upstream}/\alpha_{downstream}$	T at the midpoint (L=80m)	Midpoint width (L=80m)	T at the midpoint (L=100m)	Midpoint width (L=100m)
4-1	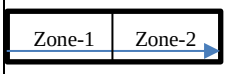	0.5	47.2	1.6	58.2	2.1
4-2	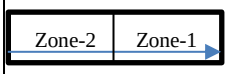	2	48.8		60.3	
5-1	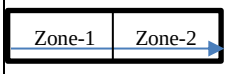	0.25	45.7	4.5	55.5	6.1
5-2	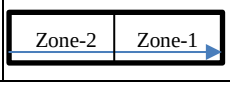	4	50.2		61.6	

The BTCs and midpoint widths of both cases show that a higher ratio of dispersivity will cause more discrepancy of BTCs. When reversing the two zones positions, the relative concentration takes less time to reach its asymptotic value with the flux flows from the lower dispersivity zone to the higher dispersivity zone. The BTCs for 4 cases from left to right are with the dispersivity ratios of 4, 2, 0.5, 0.25, respectively, it does not show a clear trend of the relative concentration at a given time. The reason of this phenomenon will discuss in section 4.4.

Retardation factor influence

In cases 6 and 7, the retardation factors are the only different parameters in two zones. In case 6, the ratio of retardation factor in zone-2 to zone-1 is 2, and in case 5 such a ratio is 4. Fig.6 shows the BTCs for cases 6 and 7 and their heterogeneity reversed situation at L=80m and L=100m.

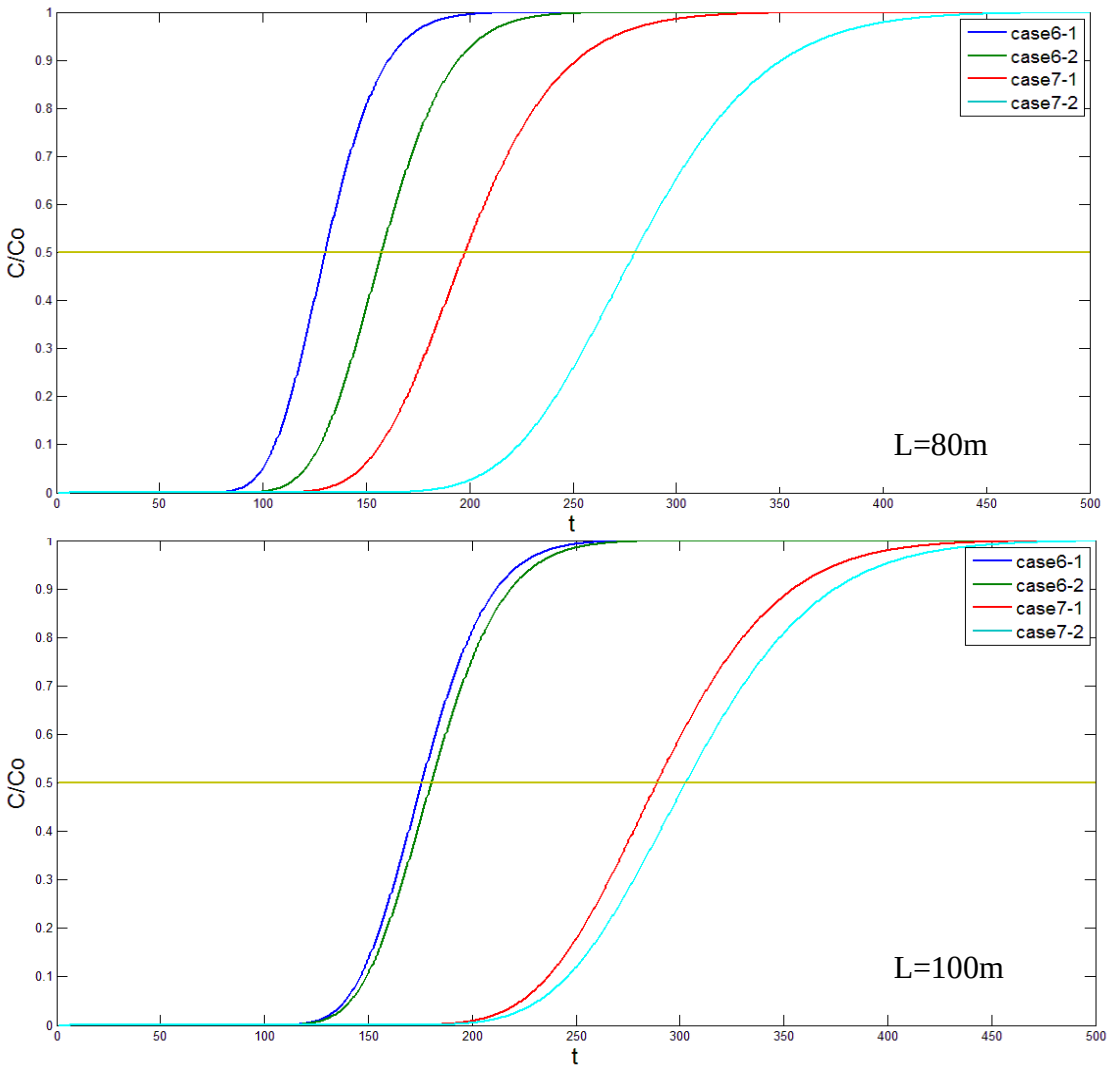

Figure 6. BTCs for cases 6-7 at L=80m and L=100m, where dash 1means flow direction is from zone-1 to zone-2, and dash 2 means flow direction is from zone-2 to zone-1.

Table 5. Transport situations for cases 6-7(retardation factor difference).

Case No.	Flow direction	$R_{upstream}/R_{downstream}$	T at the midpoint (L=80m)	Midpoint width (L=80m)	T at the midpoint (L=100m)	Midpoint width (L=100m)
6-1	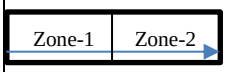	0.5	130.2	27.5	176.1	4.5
6-2	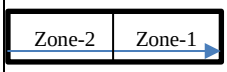	2	157.7		180.6	
7-1	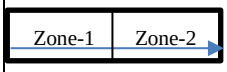	0.25	197.6	82.3	288.9	14.0
7-2	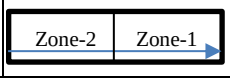	4	279.9		302.9	

The BTCs and midpoint widths of both cases show that when the ratio of retardation factors increases, the influence of solute transport increases when the order of heterogeneity reverses. When reversing the two zones' positions, the relative concentration takes less time to reach its asymptotic value with the flux flows from the zone with a lower retardation factor to the zone with a higher retardation factor. The retardation factor reflects sorptive process, which slows down the transport of a solute in the aqueous phase through a porous media. In case 6-1, zone-1 has a lower retardation factor, which means that the solute will reach the interface of zone-1 and zone-2 faster than that in case 6-2, and zone-2 will have a higher concentration than that in case 6-2 at a given time. When the time is long enough, the relative concentration will reach 1.0.

Reaction rate influence

In cases 8 and 9, the reaction rates are the only different parameter in two zones. In case 8, the ratio of reaction rate in zone-2 to zone-1 is 2, and in case 5 such a ratio is 4. Fig.7 shows the BTCs for cases 8 and 9 and their heterogeneity reversed situation at L=80m and L=100m.

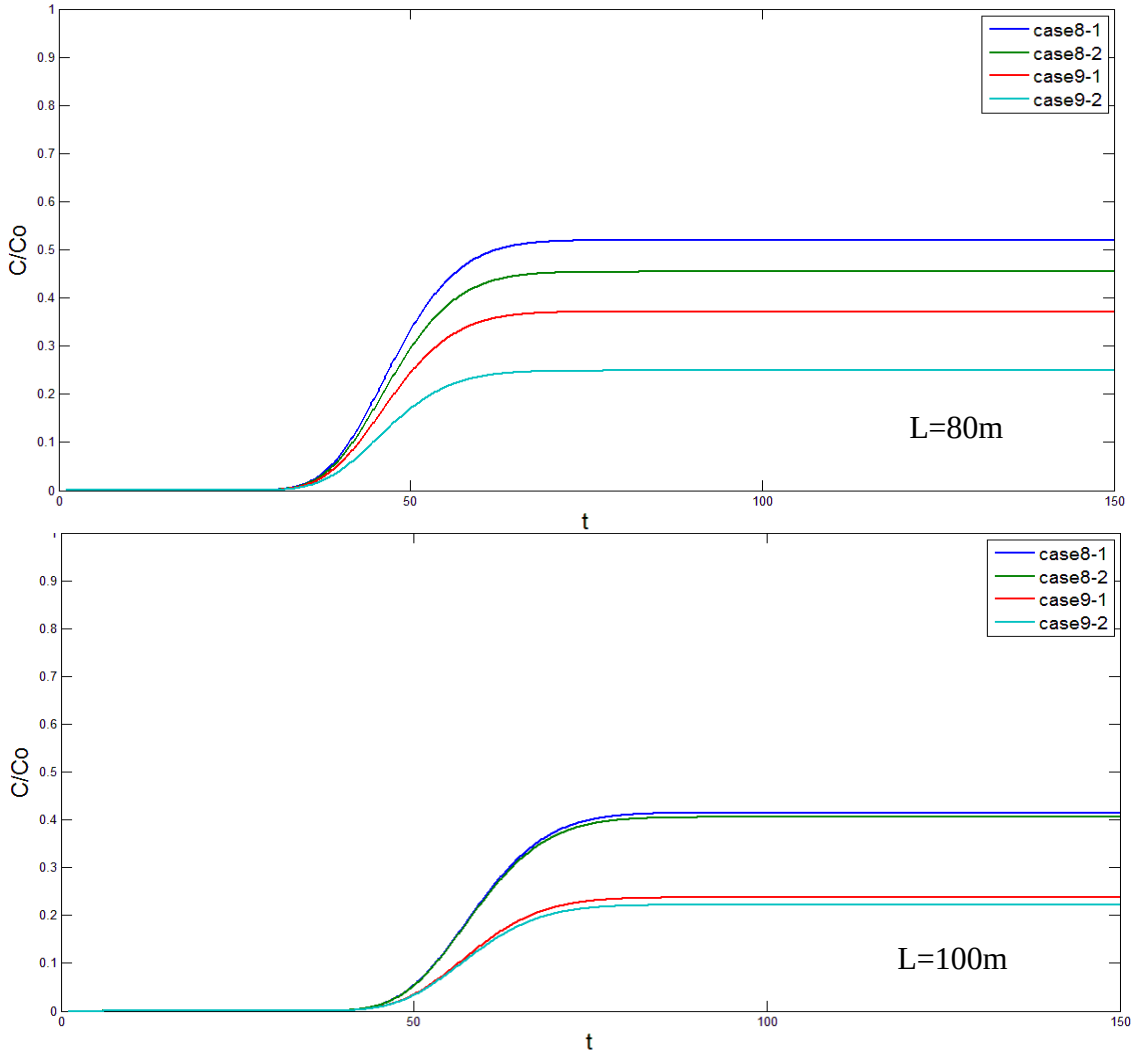

Figure 7. BTCs for cases 8-9 at L=80m and L=100m, where dash 1means flow direction is from zone-1 to zone-2, and dash 2 means flow direction is from zone-2 to zone-1.

Table 6. Transport situations for cases 8-9 (reaction rate difference).

Case No.	Flow direction	$\lambda_{upstream}/\lambda_{downstream}$	T at the C/C_0=0.2 (L=80m)	Width (L=80m)	T at the C/C_0=0.2 (L=100m)	Width (L=100m)
8-1	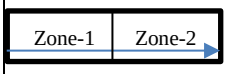	0.5	45.2	0.9	58.1	0.3
8-2	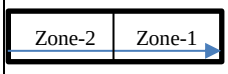	2	46.1		58.4	
9-1	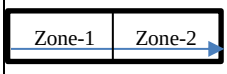	0.25	47.6	5.4	66.6	2.3
9-2	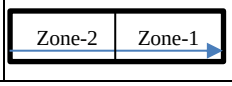	4	53.0		68.9	

The BTCs and the widths between t at C/C_0=0.2 of both cases show that when the ratio of reaction rate increases, the influence of solute transport increases when the order of heterogeneity reverses. Among all cases, the reaction rate difference appears to have the least influence when the order of heterogeneity reverses. When reversing two zones' positions, the relative concentration is higher with the flow direction from a lower reaction rate zone to a higher reaction rate zone (cases 8-1 and 9-1). As the porosity, dispersivity, retardation factors are the same for zone-1 and zone-2, the groundwater flow velocities are the same in these two zones, and the relative concentrations take almost the same time to reach their asymptotic values when the order of heterogeneity reverses. When the transport time is nearly same, a higher reaction rate in zone-1 means a lower concentration in the interface of zone-1 and zone-2, which is shown in case 9-2.

Length of zone influence

For cases 10-12, I change the relative lengths of zone-1 and zone-2 but keep the total length fixed at 100m. The same transport properties have been used for cases 10-12 with the exception that different lengths of zone-1 and zone-2 are involved. Fig.8 shows the BTCs for cases 10-12 and their heterogeneity reversed situation at L=100m. Cases 13-15 are used to further check the conclusions made in cases 10-12. Similar to cases 10-12, the relative lengths of zone-1 and zone-2 are changed but the total length of zone-1 and zone-2 remains at 100m in cases 13-15. Meanwhile, the same transport properties have been used for cases 13-15, similar to what has been done in cases 10-12. However, the parameter values used in cases 13-15 are different from those in cases 10-12. For example, the porosity is 0.15 in zone-1 and 0.3 in zone-2 in cases 10-12, while it is 0.3 in both of zone-1 and zone-2 in cases 13-15; dispersivity is 4m in zone-1 and 1m in zone-2 in cases 10-12, while it is 2m in zone-1 and 3m in zone-2 in cases 13-15; the retardation factor is 3 in zone-1 and 2 in zone-2 in cases 10-12 and it is 2 in zone-1 and 1.5 in zone-2 in cases 13-15; the reaction rate is 0 in cases 10-12, while it is 0.01 day^{-1} in zone-1 and 0.02 day^{-1} in zone-2 in cases 13-15. Fig.9 shows the BTCs for cases 13-15 and their heterogeneity reversed situation at L=100m.

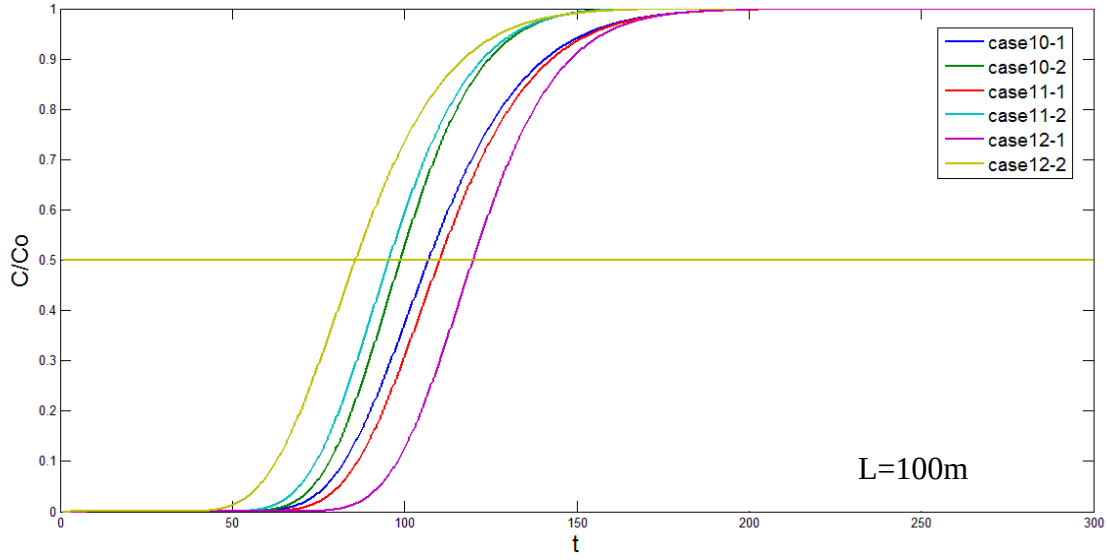

Figure 8. BTCs for cases 10-12 at L=100m, where dash 1means flow direction is from zone-1 to zone-2, and dash 2 means flow direction is from zone-2 to zone-1.

Table 7. Transport situations for cases 10-12(porosity, dispersivity, retardation factor, and length of zone difference).

Case No.	Flow direction	$L_{upstream}/L_{downstream}$	T at the midpoint (L=100m)	Midpoint width (L=100m)
10-1	Zone-1 Zone-2	1	107.1	8.3
10-2	Zone-2 Zone-1	1	98.8	
11-1	Zone-1 Zone-2	0.67	110.1	14.6
11-2	Zone-2 Zone-1	1.5	95.5	
12-1	Zone-1 Zone-2	0.11	120.0	34.1
12-2	Zone-2 Zone-1	9	85.9	

The BTCs and width of midpoints for cases 10-12 show that the midpoint width increases with the length difference between zone-1 and zone-2 increasing when the order of the heterogeneity reverses.

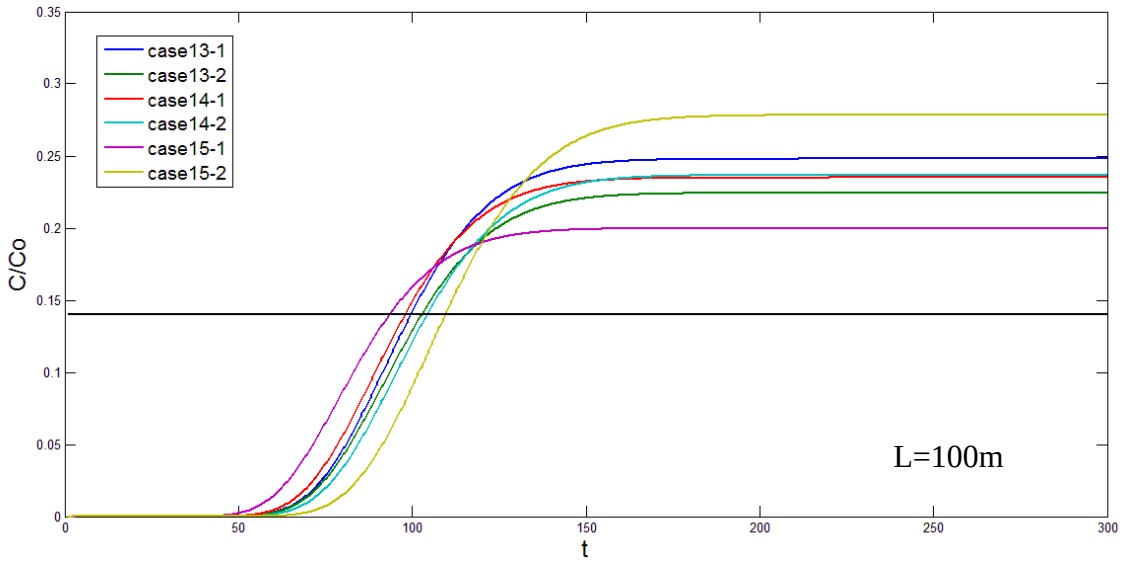

Figure 9. BTCs for cases 13-15 at *L*=100m, where dash 1means flow direction is from zone-1 to zone-2, and dash 2 means flow direction is from zone-2 to zone-1.

Similar conclusions can be drawn from cases 13-15 as for cases 10-12. When the difference between two zone length increases, the difference between asymptotic values of relative concentration also increases, which shows in Table 8.

Table 8. Transport situations for cases 13-15 (dispersivity, retardation factor, reaction rate, and length of zone difference).

Case No.	Flow direction	$L_{upstream}$ $/L_{downstream}$	T at the C/C_0=0.14 (L=100m)	Width (L=100m)
13-1	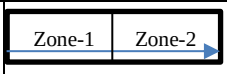	1	99.7	3.2
13-2	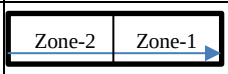	1	102.9	
14-1	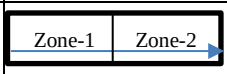	0.67	100.0	4.4
14-2	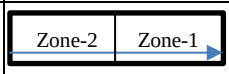	1.5	104.4	
15-1	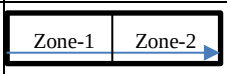	0.11	93.7	15.8
15-2	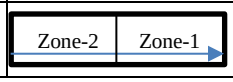	9	109.5	

The above results illustrates that the difference of retardation factor (R_i), dispersivity (α_i), porosity (θ_i), reaction rate (λ_i) and length of zones will affect the contaminant transport and concentration in the system when the order of heterogeneity reverses and the influence will increase when the difference of parameters between these two zones increases. For cases 2-9, lower values of porosity, dispersivity, and retardation factor of zone-1 will lead to the relative concentrations arriving their asymptotic limits faster, and a lower reaction rate of zone-1 will lead to a higher asymptotic value for the relative concentration. For cases 10-15, the difference between the BTCs increases with the difference between lengths of two zones increasing.

4.3 Homogenization of Parameter

It is desirable to approximate a heterogeneous two-zone system using a homogenized system with averaged transport parameters if one is permitted to do so. This is partially because it is much easier to deal with a homogeneous system rather than a heterogeneous system. This section is developed to calculate the approximate averaged parameters after media homogenization of cases 2-15 discussed in section 4.2.

The homogenization is a mathematically method to analyze the equivalent behavior of flow transport in subsurface through heterogeneous media. The basic idea of homogenization is to find the least squares to fit a set of real world observation values with a model that is non-linear with several unknown parameters.

Given input date set *X* and the observed output data set *Y*, the coefficients *x* could be found by

$$\min_x \left\| F\left(x, X\right) - Y \right\|_2^2 = \min_x \sum_i \left(F\left(x, X_i\right) - Y_i \right)^2 \tag{4-1}$$

where *X* and *Y* are matrices and *F*(*x*, *X*) is a matrix-valued function of the same size as *Y*.

Used MATLAB least squares fitting curve function to solve this problem and the MATLAB script is in Appendix B.

‘[x, resnorm, residual] =lsqcurvefit (fun, x0, X, Y)’ (4-2)

where ‘fun’ is the non-linear model.

The homogenization is done using the following procedures. Firstly, use the averaged value of parameter as the initial predicted solution (x_0) for MATLAB least squares fitting curve function. Secondly, set the time as *X* and the calculated results from cases 2-15 in section 4.2 as *Y*; use the analytical solution from section 3 as the nonlinear

function fun(x, X) with identical transport parameters for zone-1 and zone-2. Thirdly, start at x_0 to calculate unknown parameter x to best fit the fun(x, X) with the data set Y in the least-squares sense.

From the solution of Laplace inverse transform in section 3.1, the variables of solutions are $t_D = \frac{D_1}{L^2}t$, $x_D = \frac{x}{L}$, $P_{e1} = \frac{v_1 L}{D_1}$, $P_{e2} = \frac{v_2 L}{D_2}$, $\beta = \frac{D_2}{D_1}$, $\lambda_{1D} = \frac{\lambda_1 L^2}{D_1}$, $\lambda_{2D} = \frac{\lambda_2 L^2}{D_2}$, R_1, R_2, $\mathrm{L}_{1D} = \frac{L_1}{L}$, and $\gamma = \frac{\theta_2}{\theta_1} = \frac{v_1}{v_2}$. When conducting the homogenization of porous media, the transport properties are the same of two zones, so we got $\beta = \gamma = x_D = L_{1D} = 1$. Then R, $t_D = \frac{D}{L^2}t$, $P_e = \frac{vL}{D}$, and $\lambda_D = \frac{\lambda L^2}{D}$ will be the fitting parameters. Through the results of fitting parameters, the homogenized porosity, dispersivity, retardation factor and reaction rate could be found.

Homogenization of porosity

Cases 2 and 3 are used to do the homogenization of porosity. All the transport properties between two zones in case 2 are the same except for porosity, so as the case 3. Fig.10 shows the BTCs obtained in section 4.2 and the BTCs obtained using the fitting porosity.

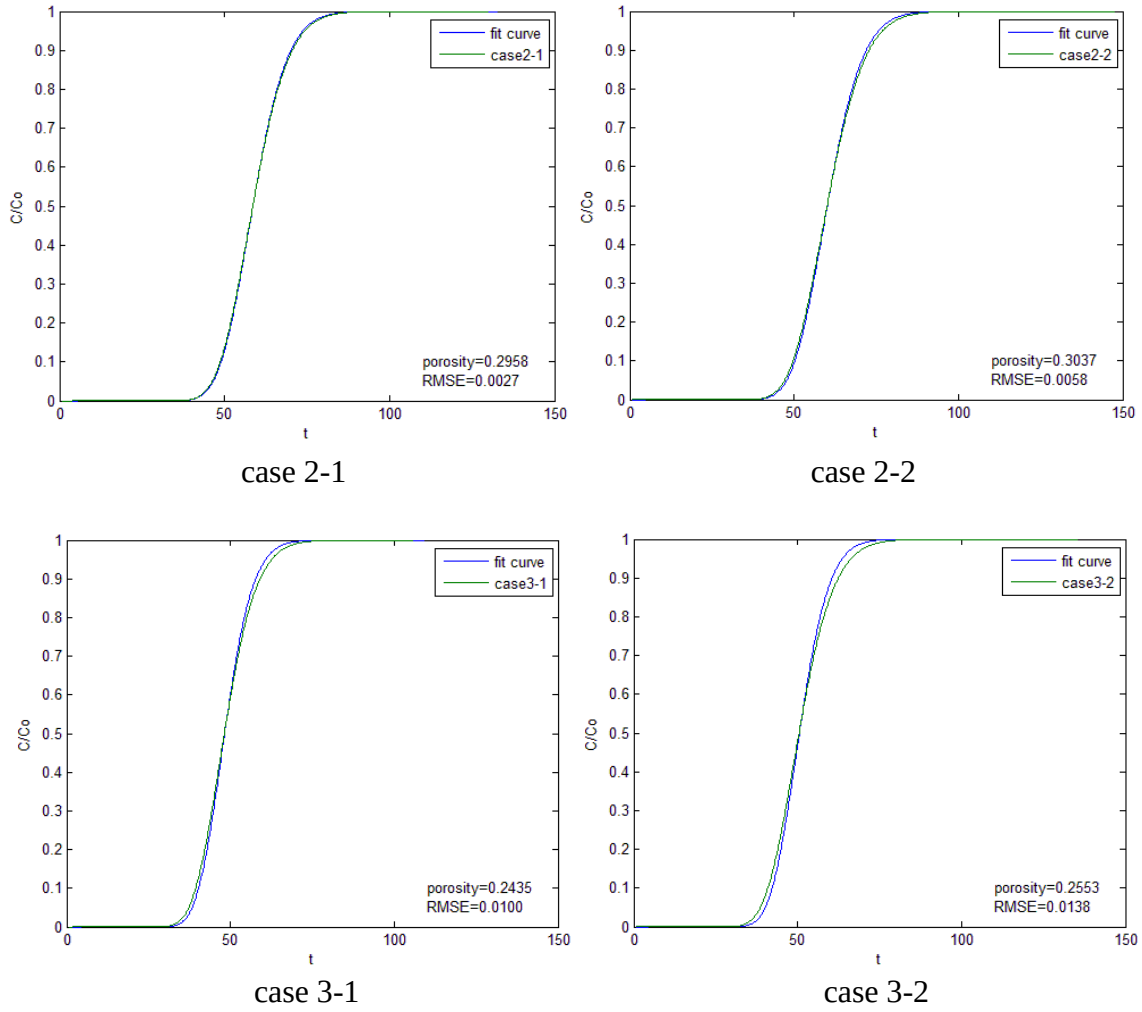

Figure 10. The BTCs of homogenized system and original heterogeneous system at the end of column (L=100m) for cases 2-3.

Table 9. Transport properties and homogenization results for cases 2-3.

Case No.	Flow direction	θ_1	θ_2	$\theta_{upstream}$ /$\theta_{downstream}$	Homogenized value	RMSE
2-1	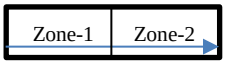	0.2	0.4	0.5	0.296	0.0027
2-2	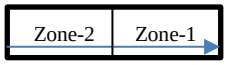	0.2	0.4	2	0.304	0.0058
3-1	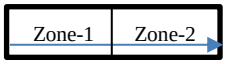	0.1	0.4	0.25	0.243	0.0100
3-2	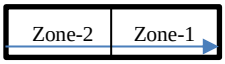	0.1	0.4	4	0.255	0.0138

The results show that the homogenized porosity will be smaller when the flow direction is from low porosity zone to high porosity zone ($\frac{\theta_{upstream}}{\theta_{downstream}} < 1$). The homogenized value is close to the arithmetic average of the parameter values of two zones. From RMSE values, the homogenized values appear to be less accurate and the BTCs of fitting parameter fit with BTCs of original parameter poorer when the ratio of porosities between two zones increases.

Homogenization of dispersivity

Cases 4 and 5 are used to do the homogenization of dispersivity. All the transport properties between two zones in case 4 are the same except for dispersivity, so as the case 5. From the fitting parameter $t_D = \frac{D}{L^2}t$, homogenized dispersivity could be found. Fig.11 shows the BTCs obtained in section 4.2 and the BTCs got using the fitting dispersivity.

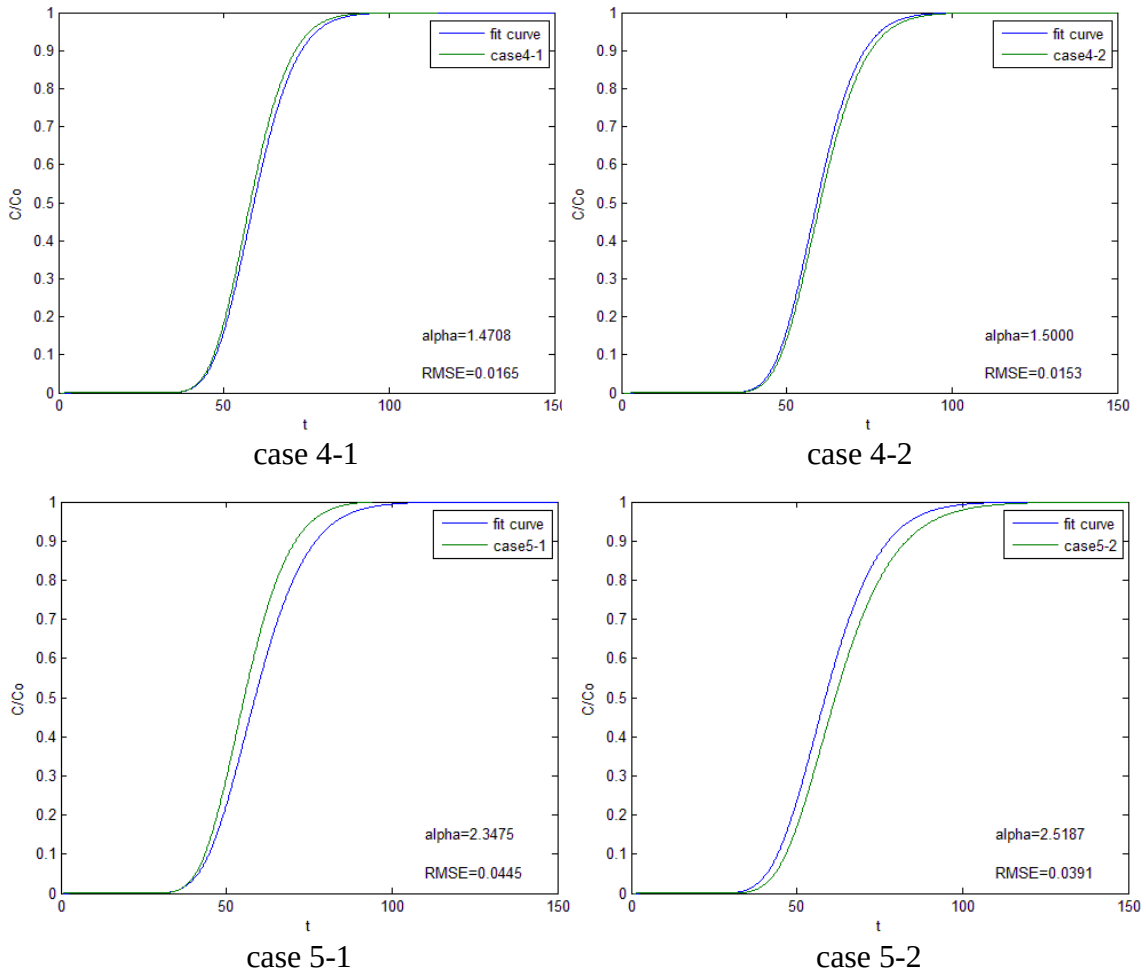

Figure 11. The BTCs of homogenized system and original heterogeneous system at the end of column (L=100m) for cases 4-5.

Table 10. Transport properties and homogenization results for cases 4-5.

Case No.	Flow direction	α_1 (m)	α_2 (m)	$\alpha_{upstream}$ $/\alpha_{downstream}$	Homogenized value	RMSE
4-1	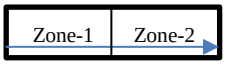	1	2	0.5	1.471	0.0165
4-2	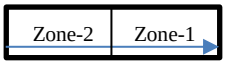	1	2	2	1.500	0.0153
5-1	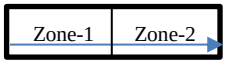	1	4	0.25	2.347	0.0445
5-2	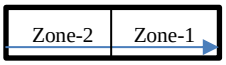	1	4	4	2.519	0.0391

The results show that the homogenized dispersivity will be smaller when the flow direction is from low dispersivity zone to high dispersivity zone ($\frac{\alpha_{upstream}}{\alpha_{downstream}} < 1$). The homogenized value is close to the arithmetic average of the parameter values of two zones. RMSE values indicate that the accuracy of homogenized values will decrease as the difference in parameter values between the two zones increases. When the ratio of dispersivity between two zones is 4, the curves fit with each other poorly. Therefore, it is difficult to homogenize the heterogeneous system using an averaged dispersivity alone when the difference of dispersivity between two zones is 4 or more.

Homogenization of retardation factor

Cases 6 and 7 are used to do the homogenization of retardation factor. All the transport properties between two zones in case 6 are the same except for retardation factor, so as the case 7. *R* is the fitting parameter that could be found directly. Fig.12 shows the BTCs obtained in section 4.2 and the BTCs calculated through fitting retardation factor.

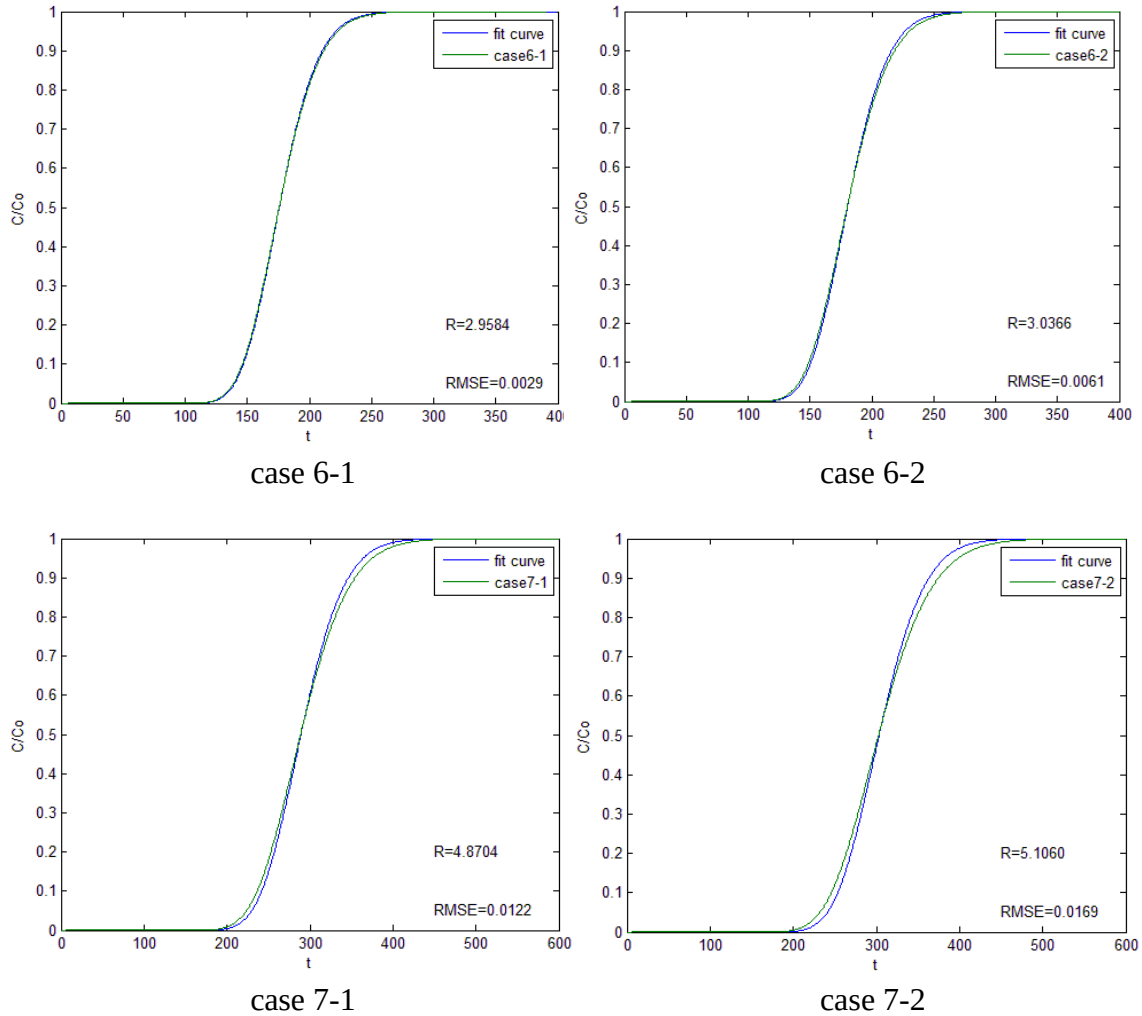

case 6-1 case 6-2

case 7-1 case 7-2

Figure 12. The BTCs of homogenized system and original heterogeneous system at the end of column (*L*=100m) for cases 6-7.

Table 11. Transport properties and homogenization results for cases 6-7.

Case No.	Flow direction	R_1	R_2	$R_{upstream}/R_{downstream}$	Homogenized value	RMSE
6-1	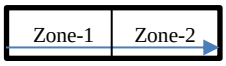	2	4	0.5	2.958	0.0029
6-2	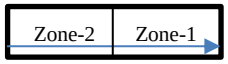	2	4	2	3.037	0.0061
7-1	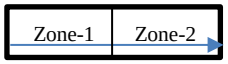	2	8	0.25	4.870	0.0122
7-2	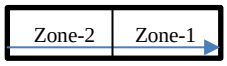	2	8	4	5.106	0.0169

The results show that the homogenized retardation factor will be smaller when the flow direction is from low retardation factor zone to high retardation factor zone ($\frac{R_{upstream}}{R_{downstream}} < 1$). The homogenized value is close to the arithmetic average of the parameter values of two zones. RMSE values indicate that the accuracy of homogenized values will decrease as the difference in retardation factor values between two zones increases. When the ratio of retardation factor between two zones is 4, the curves do not fit with each other well. Therefore, the retardation factor is difficult to homogenize when the difference of retardation factor between two zones is 4 or more.

Homogenization of reaction rate

Cases 8 and 9 are used to do the homogenization of reaction rate. All the transport properties between two zones in case 8 are the same except reaction rate, so as the case 9. From the fitting parameter $\lambda_D = \frac{\lambda L^2}{D}$, homogenized reaction rate could be found. Fig.13 shows the BTCs obtained in section 4.2 and the BTCs obtained using fitting reaction rate.

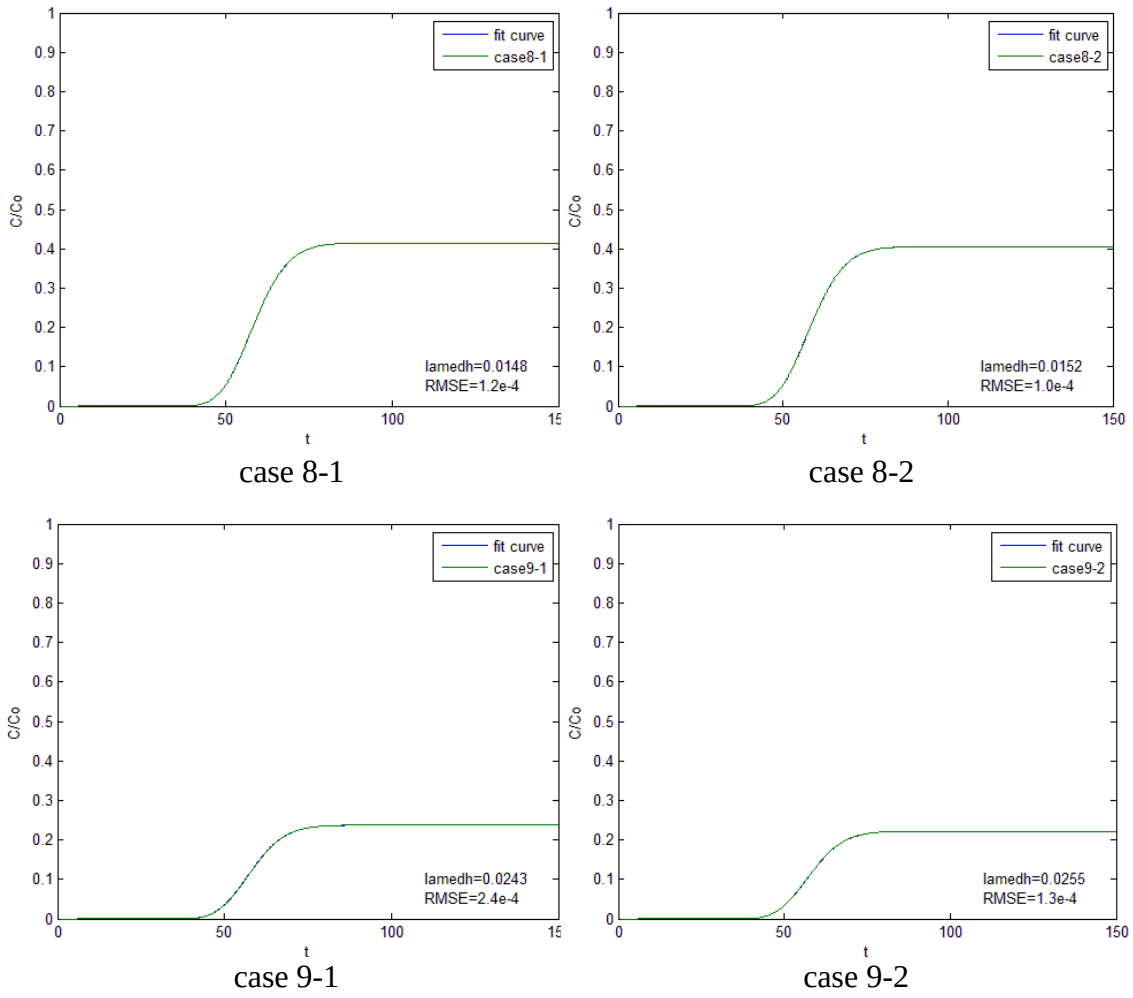

Figure 13. The BTCs of homogenized system and original heterogeneous system at the end of column (L=100m) for cases 8-9.

Table 12. Transport properties and homogenization results for cases 8-9.

Case No.	Flow direction	λ_1 (1/d)	λ_1 (1/d)	$\lambda_{upstream}$ $/\lambda_{downstream}$	Homogenized value	RMSE
8-1	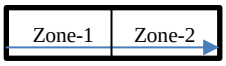	0.01	0.02	0.5	0.015	0.00012
8-2	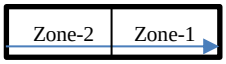	0.01	0.02	2	0.015	0.00010
9-1	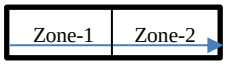	0.01	0.04	0.25	0.024	0.00024
9-2	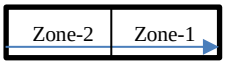	0.01	0.04	4	0.025	0.00013

The results show that the homogenized reaction rate will be smaller when the flow direction is from low reaction rate zone to high reaction rate zone ($\frac{\lambda_{upstream}}{\lambda_{downstream}} < 1$). The homogenized value is close to the arithmetic average of the parameter values of two zones. RMSE values indicate that the accuracy of homogenized reaction rate will decrease as the difference in reaction rate values between the two zones increases. When the ratio of reaction rate between two zones is 4, the curves still fit with each other very well. Therefore, the reaction rate is the easiest parameter to homogenize.

Homogenization of multi-parameter

In cases 10-12, I did the homogenization of the two-zone system with three changing parameters (porosity, dispersivity, and retardation factor). The BTCs of homogenized system and original heterogeneous system at the end of column (L=100m) are shown in Fig. 14.

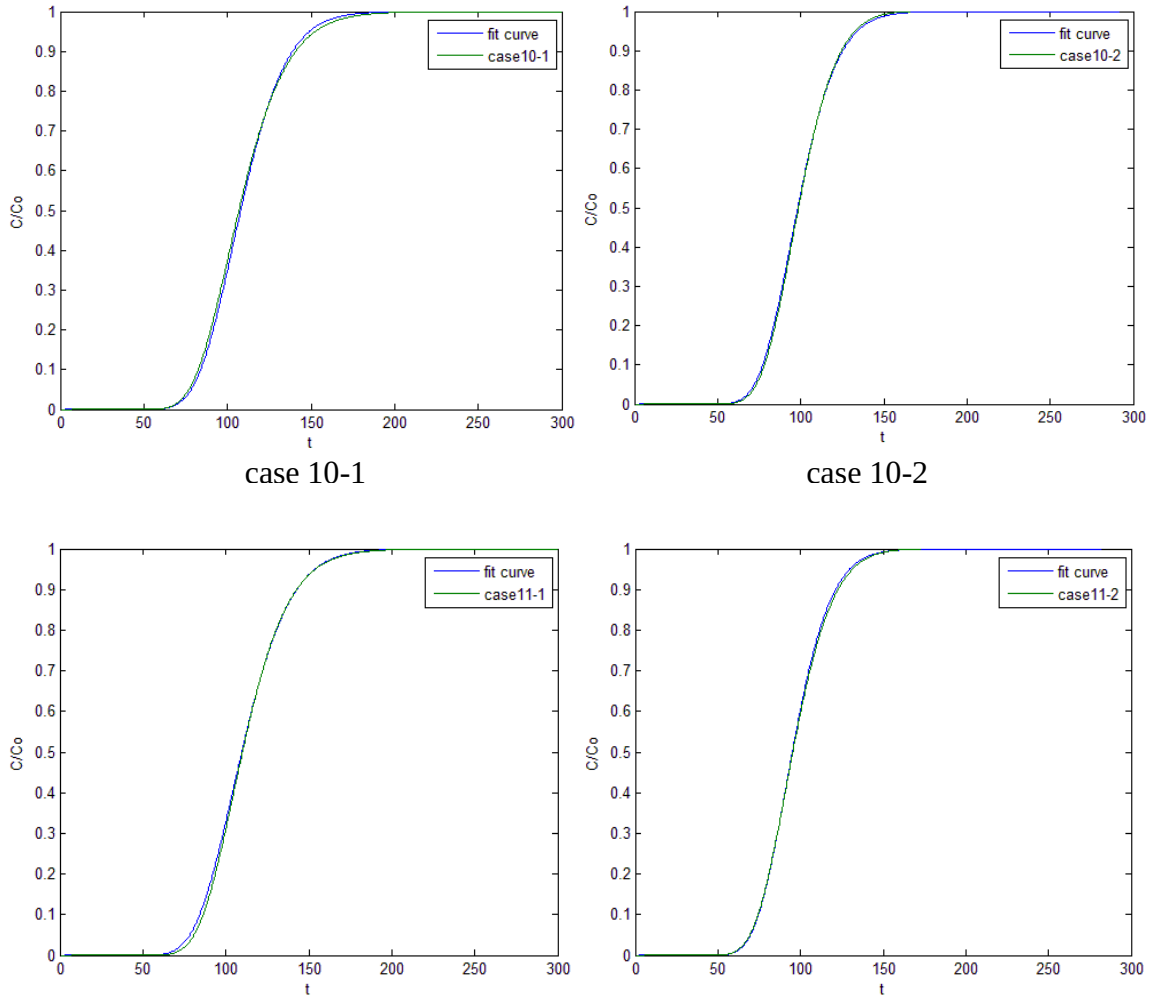

case 10-1 case 10-2

case 11-1 case 11-2

Figure 14. The BTCs of homogenized system and original heterogeneous system at the end of column (L=100m) for cases 10-12.

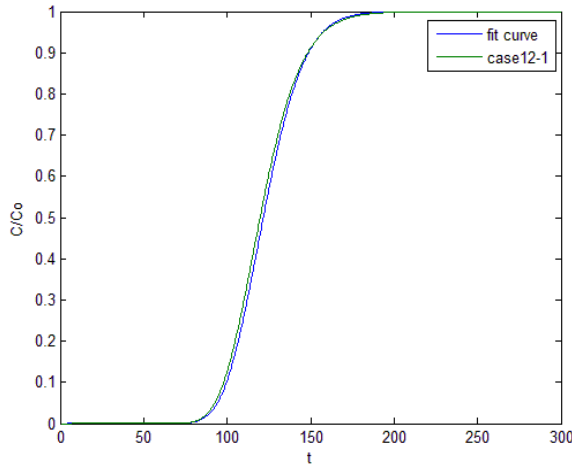

case 12-1

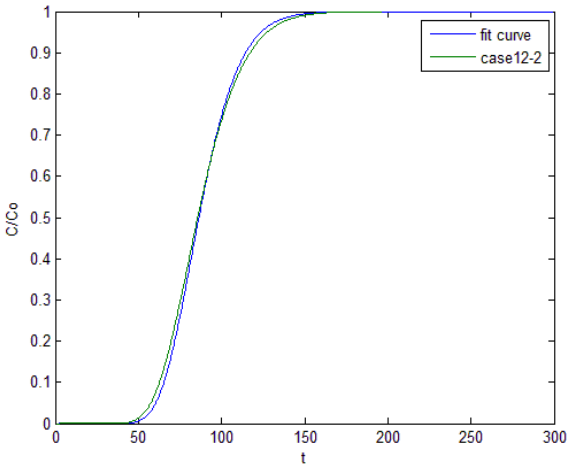

case 12-2

Figure 14. Continued.

Table 13. Transport properties and homogenization results for cases 10-12.

Case No.	Flow direction	Homogenized θ	Homogenized α (m)	Homogenized R	RMSE
10-1	Zone-1 Zone-2	0.25	2.00	2.20	0.0009
10-2	Zone-2 Zone-1	0.24	1.85	2.00	0.0005
11-1	Zone-1 Zone-2	0.28	2.20	2.00	0.0027
11-2	Zone-2 Zone-1	0.22	1.85	2.20	0.0013
12-1	Zone-1 Zone-2	0.28	1.25	2.20	0.0047
12-2	Zone-2 Zone-1	0.26	2.50	1.70	0.0010

In cases 13-15, I did the homogenization of the two-zone system with three other changing parameters (dispersivity, reaction rate, and retardation factor). The BTCs of

homogenized system and original heterogeneous system at the end of column (L=100m) shows in Fig. 15.

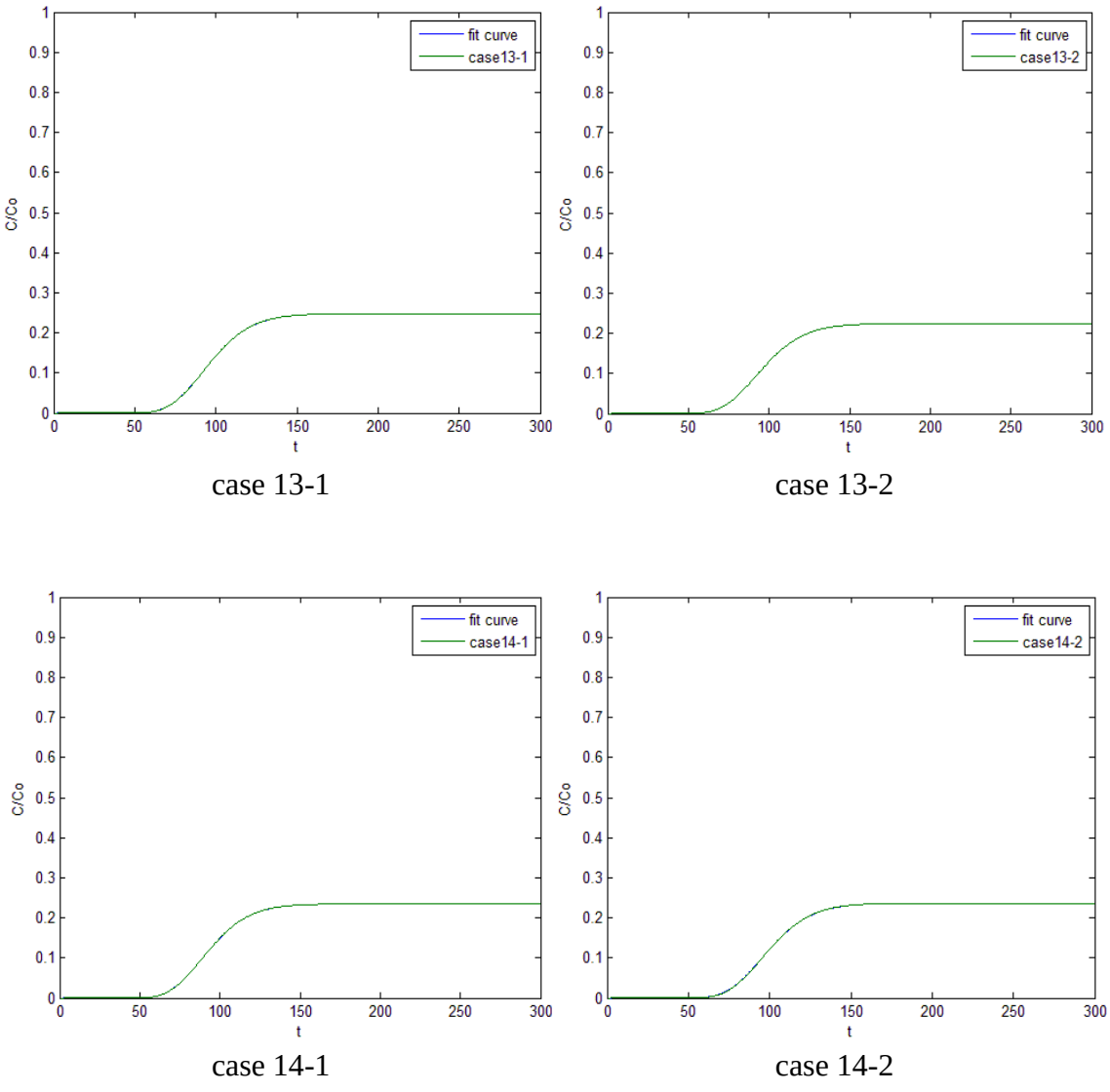

Figure 15. The BTCs of homogenized system and original heterogeneous system at the end of column (L=100m) for cases 13-15.

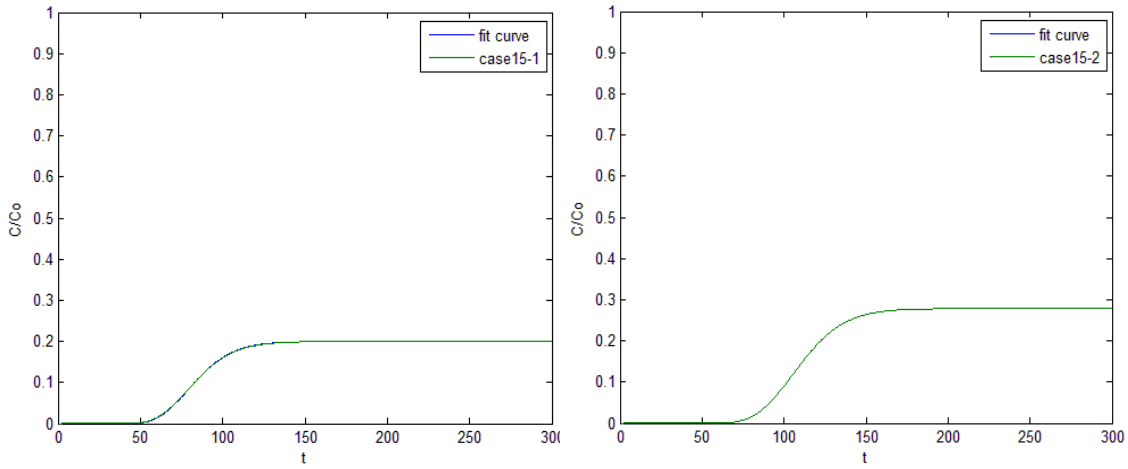

case 15-1 case 15-2

Figure 15. Continued.

Table 14. Transport properties and homogenization results for cases 13-15.

Case No.	Flow direction	Homogenized α (m)	Homogenized R	Homogenized λ	RMSE
13-1	Zone-1 Zone-2	2.40	1.74	0.0137	$5.2*10^{-5}$
13-2	Zone-2 Zone-1	2.41	1.75	0.0147	$5.4*10^{-6}$
14-1	Zone-1 Zone-2	2.50	1.70	0.0147	$3.1*10^{-5}$
14-2	Zone-2 Zone-1	2.37	1.81	0.0137	$2.2*10^{-4}$
15-1	Zone-1 Zone-2	2.65	1.53	0.0182	$5.7*10^{-4}$
15-2	Zone-2 Zone-1	2.08	1.95	0.0112	$1.2*10^{-5}$

The results show that the homogenized parameters will depend on the order of heterogeneity as discussed above. When the order of heterogeneity reverses, the

homogenized parameters change, but there is no clear trend of the homogenized parameters, which is different from cases 2-9 with single fitting parameter in the homogenization process. In cases 2-9, the homogenized parameter is always smaller when the flow direction is from low property zone to high property zone than that in the reversed situation.

Furthermore, another notable point is that the homogenized parameters are not close to the arithmetic averages of the parameter values of those two zones. In case 12-2, the homogenized retardation factor is even smaller than the minimum retardation factor value of two zones. So arithmetic average of the parameter could be used as the homogenized parameter for rough estimation in single parameter homogenization, but cannot be used in multi-parameter homogenization.

4.4 Scale-dependent Issue

The dispersion has been proved to be scale-dependent, which means the calculated dispersivity value will increase with the travel distance in a tracer test increasing (Molz et al., 1983). To investigate the scale effect and the exit boundary condition effect of dispersivity in the two-zone system, I extend the total length to 150m, 200m, and 500m, while keep the length of zone-1 to be 50m, and draw BTCs at a fixed position of x=100m in cases 16-18. The transport properties of cases 16-18 shows in Table 15.

Table 15. Transport properties of conceptual cases 16-18.

Case No.	L (m)	θ_1	θ_2	α_1 (m)	α_2 (m)	R_1	R_2	λ_1 (1/d)	λ_2 (1/d)
16	150	0.3	0.3	1	4	1	1	0	0
17	200	0.3	0.3	1	4	1	1	0	0
18	500	0.3	0.3	1	4	1	1	0	0

Two scenarios discussed in each of cases 16-18, which have different lengths for zone-1 and zone-2, requires special attention as it is different from the two scenarios discussed in each of cases 2-15, which simply switch zone-1 and zone-2. For the two scenarios in each of cases of 16-18, the position of the zone-1 and zone-2 is not switched but the value of dispersivity is switched instead. For example, the dispersivity values of zone-1 and zone-2 in case 16-1 are the same as the dispersivity values of zone-2 and zone-1 in case 16-2, respectively, but the positions of zone-1 and zone-2 remain the same in cases 16-1 and 16-2. The same is true for cases 17 and 18. The BTCs of cases 5, 16- 18 are shown in Fig. 16.

Notice that when the total length gets longer, the difference of BTCs will decrease. When the total length is longer more than 150m, the difference does not change anymore, meaning that the total length will impact the difference of BTCs for above mentioned two different scenarios, but to a much less extent.

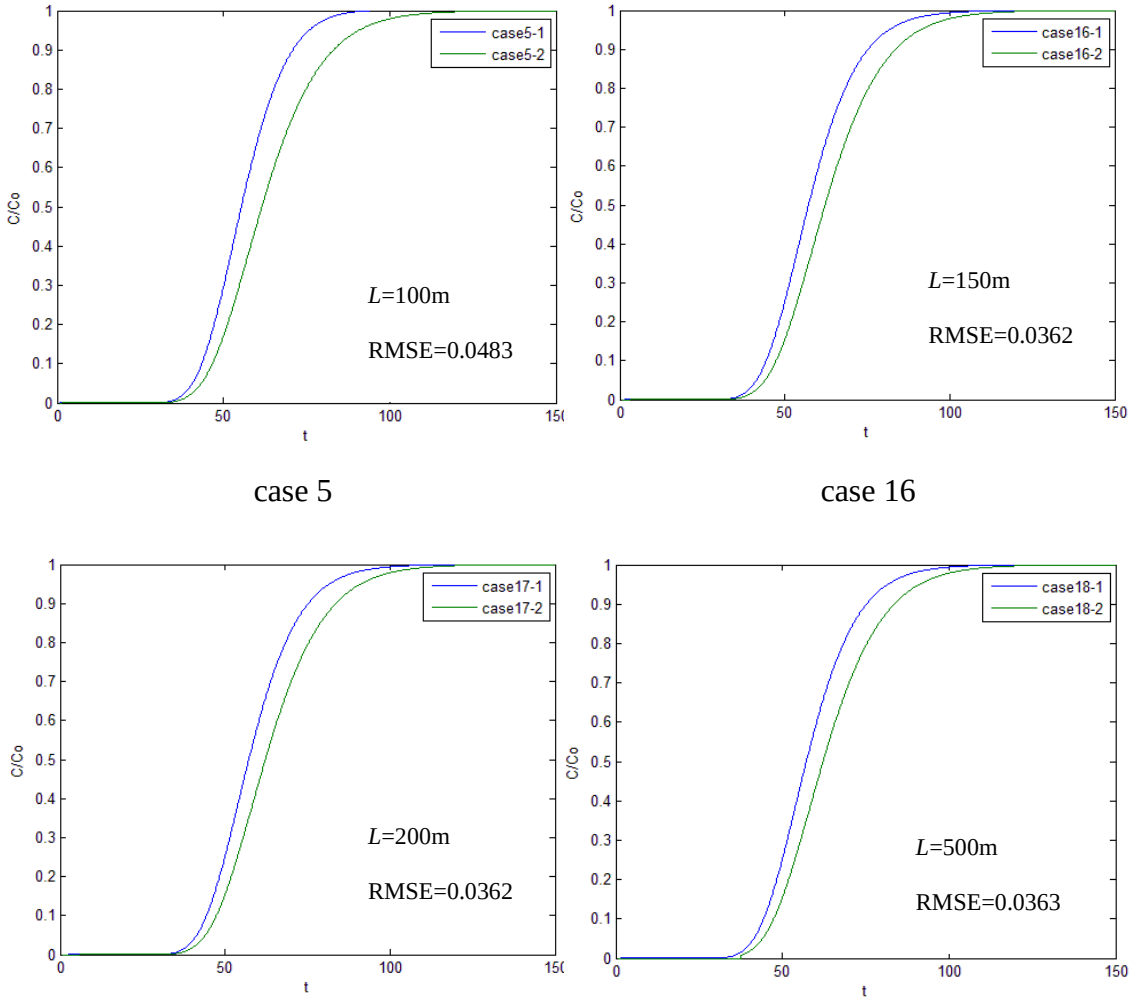

case 5 case 16

case 17 case 18

Figure 16. BTCs for cases 5, 16-18 at x=100m of the two-zone porous media.

From the above result, I assume that the homogenized result of dispersivity will change with the travel distance. Consider the cases 19-20 with different travel distances and same properties with case 4. The transport properties are shown in Table 16.

Table 16. Transport properties of conceptual cases 19-20.

Case No.	L (m)	L_1 (m)	θ_1	θ_2	α_1 (m)	α_2 (m)	R_1	R_2	λ_1 (1/d)	λ_2 (1/d)
4	100	50	0.3	0.3	1	2	1	1	0	0
19	50	25	0.3	0.3	1	2	1	1	0	0
20	10	5	0.3	0.3	1	2	1	1	0	0

Fig. 17 shows the results of homogenized parameters and the BTCs of the homogenized system and the original heterogeneous system.

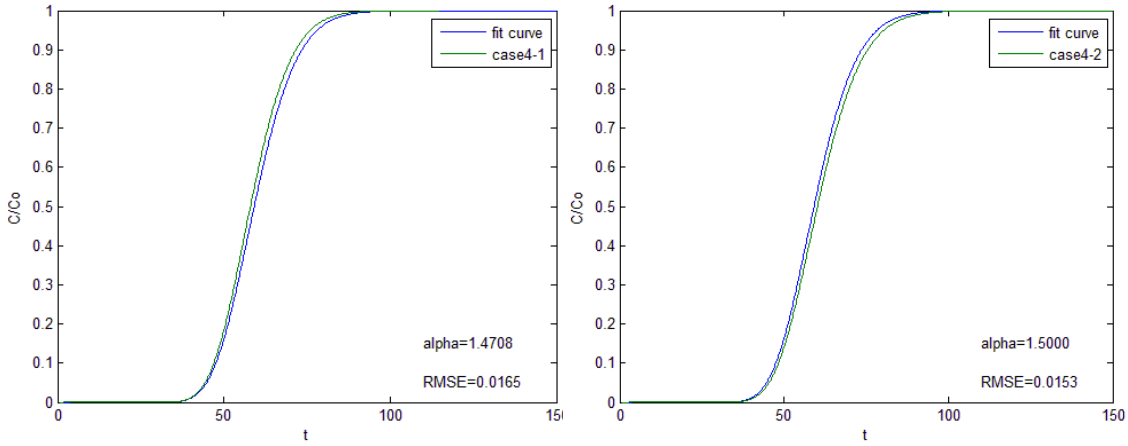

case 4-1 case 4-2

Figure 17. The BTCs of homogenized system and original heterogeneous system at the end of column for cases 19-20.

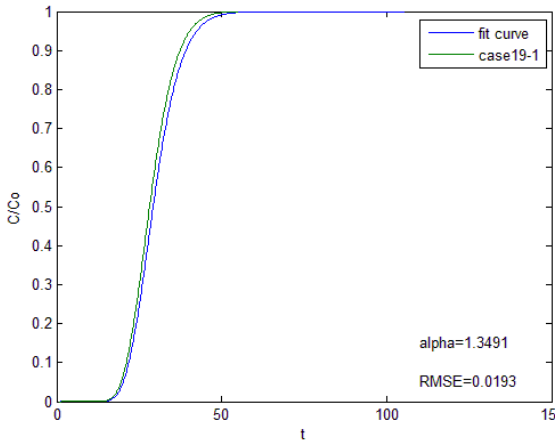

case 19-1

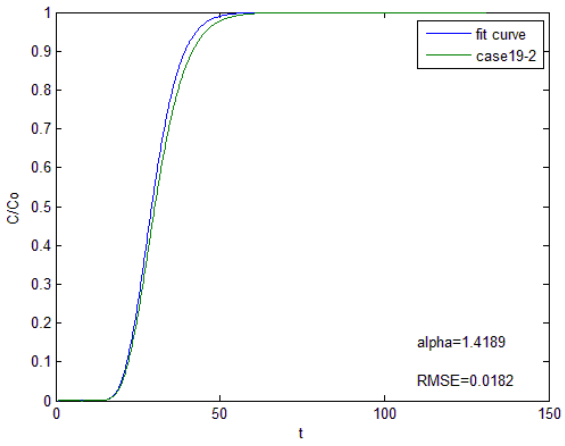

case 19-2

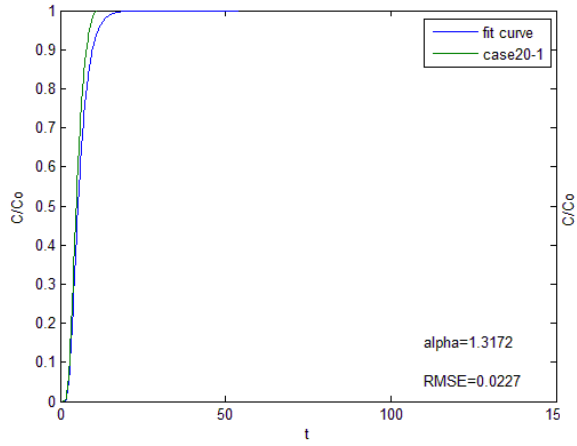

case 20-1

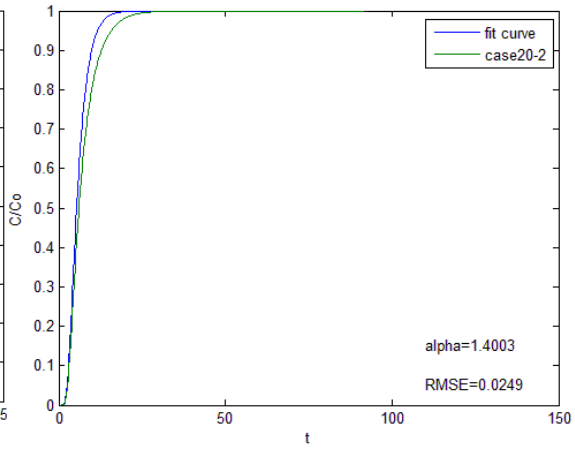

case 20-2

Figure 17. Continued.

Table 17 shows the homogenized results. Notice that the difficulty to homogenize dispersivity will increase with the travel distance decreases. When the total length is 100m, it is easy to find homogenized dispersivity values, while the total length decreases to 10m, it is hard to find homogenized dispersivity as the associated RMSE is large and the curves

fitting is poor. So the method works better when the travel distance is longer to find a homogenized dispersivity for a heterogeneous two-zone system.

Table 17. Transport properties and homogenization results for cases 19-20.

Case No.	Flow direction	L (m)	L_1 (m)	$\alpha_{upstream}$ /$\alpha_{downstream}$	Homogenized value	RMSE
4-1	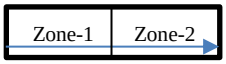	100	50	0.5	1.4708	0.0165
4-2	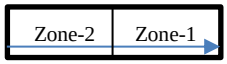	100	50	2	1.500	0.0153
19-1	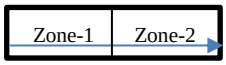	50	25	0.5	1.3491	0.0193
19-2	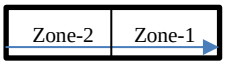	50	25	2	1.4189	0.0182
20-1	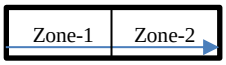	10	5	0.5	1.3172	0.3227
20-2	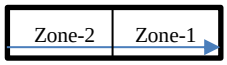	10	5	2	1.4003	0.3249

5. CONCLUSIONS

In this thesis, the semi-analytical solutions of ADE with different transport properties, first-order reaction and linear sorption has been investigated to describe the solute transport in a heterogeneous two-zone system. The focus of this thesis is on the order of heterogeneity influence, parameter difference influence, and homogenization of parameters.

The problem is first solved in Laplace domain and the real time solution is obtained using the de Hoog inverse Laplace transform. A MATLAB program is generated facilitate the computation. Then the parameter homogenization has been done by finding a constant value for one parameter of concern (such as dispersivity) for an equivalent homogenous media to approximate the heterogeneous two-zone system with different values for the same parameter of concern by best-fitting BTCs of the equivalent homogenous media to BTCs of the heterogeneous two-zone system. The parameter homogenization can be applied for a single parameter of concern or for multiple parameters of concern simultaneously.

The research mainly obtained the following conclusions. Firstly, it has been proven that the order of heterogeneity will affect the contaminant transport in the two-zone system considerably. This will give some suggestions for the real world contamination remediation. For instance, the direction of groundwater flow can be changed through digging pumping well or injection well at the special locations. As the flow direction changes, the concentration at the target position may be lower or higher than before. The

underlying zone in waste disposal fields could be two-zone system as we discussed above. When selecting the site of waste disposal, we could consider the order of heterogeneous zones in the subsurface to find out which situation could block more contamination to the groundwater.

Secondly, the results illustrates that the difference of retardation factor (R_i), dispersivity (α_i), porosity (θ_i), reaction rate (λ_i), and zone lengths between each zone will affect the contaminant transport and concentration in the system when the order of heterogeneity reverses and the influence will increase with the difference between two zone parameters increasing. This means when choosing the sites of industry or waste disposal, we could compared the transport properties and thickness of heterogeneous zones and build a natural barrier system for contamination transport.

Thirdly, when there is only one parameter need to be homogenized, the accuracy of homogenization will decrease with the difference between two zone parameters increasing. When the zone with a lower property value is upstream of the zone with a higher property value zone, the homogenized parameter will be smaller. The homogenized parameter is close to the arithmetic average of the parameters between two zones. Dispersivity has the greatest influence on the results of BTCs and it is also the most difficult one to be homogenized. The reaction rate has the least influence on the results of BTCs and it is also the easiest one to be homogenized. Furthermore, this method is better using for homogenization of dispersivity of large scale situation.

Fourthly, when there are multiple parameters to be homogenized simultaneously, the homogenized parameters change with the order of heterogeneity. But the homogenized

solutions are not close to the arithmetic averages of parameters, which is even out of the range bounded by the parameter values of two zones. Therefore, the homogenization of multiple parameters in a heterogeneous systems must be simulated by some method.

Some of the conclusions in this thesis can be used for the field situations, and related future studies will be summarized in the final section.

6. FUTURE WORK

In this thesis, there are still some issues need to be resolved in the future.

The reason that the homogenized dispersivity is different when the order of heterogeneity reverses is still unclear and deserves some detailed analysis, as this may fundamentally change our present approach of dealing with spatial heterogeneity. At present, most hydrologists believe that it is the statistical structure of spatial heterogeneity, not the actual spatial locations, determines the macroscopic (or homogenized) transport parameters such as dispersivity.

This study is based on a rather simple two-zone heterogeneous system. Therefore, whether or not the conclusions drawn here can be applied for three or more zones, requires further clarification. This study deals with a one-dimensional heterogeneous system, thus whether or not the conclusions drawn can be applied to problems with a higher dimension is also unclear.

The homogenization of parameter is dependent on the curve fitting of BTCS, which use the initial estimated valued to find the unknown parameter with the sum of the absolute values of the deviation between the approximate curve and observed curve minimized. The accuracy of fitting result is relative to the initial estimated value in some extent. There is still room for improvement for this method.

Furthermore, the laboratory and field experiments need to be established to verify the validity and accuracy of this method when using in the real world problems.

REFERENCES

Adams, E. E., and Gelhar, L. W., 1992. Field study of dispersion in a heterogeneous aquifer: 2. Spatial moments analysis. Water Resources Research, 28(12), 3292-3307.

Al-Niami, A.N.S., and Rushton, K.R., 1979. Dispersion in stratified porous media: Analytical solutions. Water Resource Research, 15(5), 1044-1048.

Amaziane, B., Bourgeat, A., and Koebbe, J., 1991. Numerical simulation and homogenization of two-phase flow in heterogeneous porous media. Transport in Porous Media, 6, 519-547.

Barry, D. A. and Parker, J. C., 1987. Approximations for solute transport through porous media with flow transverse to layering. Transport in Porous Media, 2, 65-82.

Bear, J., 1972. Dynamics of fluid in porous media. Elsevier, New York.

Benson, D. A., Wheatcraft, S. W., and Meerschaert, M. M., 2000. Application of a fractional advection-dispersion equation. Water Resources Research, 26(6), 1403-1412.

Benson, D. A., and Meerschaert, M. M., 2009. A simple and efficient random walk solution of multi-rate mobile/immobile mass transport equations. Advances in Water Resources, 32(4), 532-539.

Berkowitz, B., Cortis, A., Dentz, M., and Scher, H., 2006. Modeling non-Fickian transport in geological formations as a continuous time random walk. Reviews of Geophysics, 44(2), RG2003.

Boupha, K., Jacobs, J. M., and Hatfield, K., 2004. MDL Groundwater software: Laplace transforms and the De Hood algorithm to solve contaminant transport equations. Computers & Geosciences, 30, 445-453.

Crank, J., 1975. The mathematics of diffusion. Clarendon Press, Oxford.

Danckwerts, P. V., 1953. Continuous flow systems distribution of residence time. Chemical Engineering Science, 2(1), 1-13.

Durlofsky, L. J., 1991. Numerical calculation of equivalent grid block permeability tensors for heterogeneous porous media. Water Resources Research, 27(5), 699-708.

Ervin, V.J. and Roop, J. P., 2006. Variational formulation for the stationary fractional advection dispersion equation. Numerical Methods for Partial Differential Equations, 22(3), 558-576.

Foose, G. J., Benson, C. H., and Edil, T. B., 2002. Comparison of solute transport in three composite liners. Journal of Geotechnical and Geoenvironmental Engineering, 128(5), 590-601.

Freeze, R. A. and Cherry, J. A., 1979. Groundwater. Englewood Cliffs: Prentice Hall, New Jersey.

Freyberg, D. L., 1986. A natural gradient experiment of solute transport in a sand aquifer, 2, Spatial moments and the advection and dispersion of nonreactive tracers. Water Resources Research, 22(13), 2031-2046.

Gelhar, L. W., 1993. Stochastic subsurface hydrology. Englewood Cliffs: Prentice Hall, New Jersey.

Gelhar, L. W., and Axness, C. L., 1983. Three-dimensional stochastic analysis of macrodispersion in aquifers. Water Resources Research, 19, 161-180.

Gelhar, L. W., Welty, C., and Rehfeldt, K. R., 1992. A critical review of data on field-scale dispersion in aquifer. Water Resources Research, 28(7), 1955-1974.

Haggerty, R., and Gorelick, S. M., 1995. Multiple-rate mass transfer for modeling diffusion and surface reactions in media with pore-scale heterogeneity. Water Resources Research, 31(10), 2383-2400.

Hatfield, K., Burris, D.R., and Wolfe, N.L., 1996. Analytical model for heterogeneous reactions in mixed porous media. Journal of Environmental Engineering, 122(8), 676-684.

Hatfield, K. and Stauffer, T.B., 1993. Transport in porous media containing residual hydrocarbon. I: model. Journal of Environmental Engineering, 119(3), 540-558.

Hazardous Waste Consultant, 1996, Remediation soil and sediment contaminated with heavy metals, Elsevier Science, Netherlands.

Held, R., Attinger, S., Kinzelbach, W., 2005. Homogenization and effective parameters for the Henry problem in heterogeneous formations. Water Resources Research, 41, W11420.

Herschy, R. W. and Fairbridge, R. W., 1998. Encyclopedia of hydrology and water resources. Springer Science & Business Media, the Netherlands.

Hollenbeck, K. J., 1998. INVLAP.M: A matlab function for numerical inversion of Laplace transforms by the de Hoog algorithm, http://www.isva.dtu.dk/staff/karl/invlap.htm

Huyakorn, P. S., Springer, E. P., Guvanasen, V., 1986. A three-dimensional finite-element model for simulating water flow in variably saturated porous media. Water Resources Research, 22(13), 1790-1808.

Jacobson, O. H., Leij, F. J. and van Genuchten, M. T., 1992. Lysimeter study of anion transport during steady flow through layered coarse-textured soil profiles. Soil Science, 154(3), 196-205.

Korn, G. A. and Korn, T. M., 1968. Mathematical handbook for scientists and engineers. 2nd Edition, McGraw-Hill Book Company, N. Y.

Lampert, D. J., and Reible, D., 2009. "An analytical modeling approach for evaluation of capping of contaminated sediments." Soil Sediment Contaminant, 18(4), 470-488.

Leij, F. J., Dane, J. H. and van Genuchten, M. T., 1991. Mathematical analysis of one-dimensional solute transport in a layered soil profile, Soil Science Society of America Journal, 55, 944-953.

Leij, F. J., and van Genuchten, M. T., 1995. Approximate analytical solutions for solute transport in two-zone porous media. Transport in Porous Media, 18(1), 65-85.

Li, Y., and Cleall, P. J., 2011. Analytical solutions for advective-dispersive solute transport in double-layered finite porous media. International Journal for Numerical and Analytical Methods in Geomechanics, 35(4), 438-460.

Liu, C., Ball, W. P., and Ellis, J. H., 1998. An analytical solution to the one-dimensional solute advection-dispersion equation. Transport in Porous Media, 30, 25-43.

Liu, C., Szecsody, J. E. and Zachara, J. M., 2000. Use of the generalized integral transform method for solving equation of solute transport in porous media. Advances in Water Resources, 23(5), 483-492.

Liu, G. and Si, B. C., 2008. Multi-zone diffusion model and error analysis applied to chamber-based gas fluxes measurement. Agricultural and Forest Meteorology, 149(1), 169-178.

Mackay, D. M., Freyberg, D. L., and Roberts, P. V., 1986. A natural gradient experiment on solute transport in a sand aquifer 1. Approach and overview of plume movement. Water Resources Research, 22(13), 2017-2029.

Maupin, M. A., Kenny, J. F., Hutson, S. S., Lovelace, J. K., Barber, N. L., and Linsey, K. S., 2014. Estimated use of water in the United States in 2010. U.S. Geological Survey, Reston, Virginia.

McCarty, P. L., Reinhard, M., and Rittmann, B. E., 1980. Trace organics in ground water. Environmental Science & Technology, 15(1), 40-51.

Molina-Giraldo, N. Bayer, P., and Blum, P., 2011. Evaluating the influence of thermal dispersion on temperature plumes from geothermal systems using analytical solutions. International Journal of Thermal Sciences, 50(7), 1223-1231.

Molz, F. J., Guven, O., and Melville, J. G., 1983. An examination of scale-dependent dispersion coefficients. National Ground Water Association, 21(6), 715-725.

Mulligan, C. N., Yong, R. N., and Gibbs, B. F., 2001. Remediation technologies for metal-contaminated soils and groundwater: an evaluation. Engineering Geology, 60(1-4), 193-207.

Neuman, S. P., 1990. Universal scaling of hydraulic conductivities and dispersivities in geologic media. Water Resources Research, 26(8), 1749-1758.

Neuman, S. P., Winter, C. L., and Newman, C. M., 1987. Stochastic theory of field-scale Fickian dispersion in anisotropic porous media. Water Resources Research, 23(3), 453-466.

Ortan, A., Quenneville-Belair, V., Tilley, B. S., and Townsend J., 2009. On Taylor dispersion effects for transient solutions in geothermal heating systems. International Journal of Heat and Mass Transfer. 52(21-22), 5072-5080.

Park, E. and Zhan, H., 2001. Analytical solutions of contaminant transport from finite one-, two- and three-dimensional sources in a finite-thickness aquifer. Journal of Contaminant Hydrology, 53(1-2), 41-61.

Peaudecerf, G., and Sauty, J. P., 1978. Application of a mathematical model to the characterization of dispersion effects on groundwater quality, Progress in Water Technology, 10, 443-454.

Pérez Guerrero, J.S., Pimentel, L. C. G., and Skaggs, T. H., 2012. Analytical solution for the advection-dispersion transport equation in layered media. International Journal of Heat and Mass Transfer, 56(2013), 274-282.

Rajaram, H., and Gelhar, L. W., Plume scale-dependent dispersion in heterogeneous aquifers, 2. Eulerian analysis and three-dimensional aquifers. Water Resources Research, 29(9), 3261-3276.

Rao, P. S. C., Rolston, D. E., Jessup, R. E., and Davidson, J. M., 1980. Solute transport in aggregated porous media: theoretical and experimental evaluation. Soil Science Society of America Journal, 44(6), 1139-1146.

Roberts, P. V., Schreiner, J., and Hopkins, G. D., 1982. Field study of organic water quality changes during groundwater recharge in the Palo Alto Baylands. Water Research, 16(6), 1025-1035.

Rowe, R. K., Caers, C.J. and Chan, C., 1993. Evaluation of a compacted till liner test pad constructed over a granular subliner contingency zone. Canadian Geotechnical Journal, 30(4), 667-689.

Rowe, R. K., Quigley, R. M. Brachman, R. W. I., and Booker, J. R., 2004. Barrier systems for waste disposal facilities, Taylor & Francis, Oxford, U. K.

Selim, H. M., Davison, J. M. and Rao, P. S. C., 1977. Transport of reactive solutes through multi-layered soils. Soil Science Society of America Journal, 41, 3-10.

Shamir, U.Y., and Harleman, D. R. F., 1967. Dispersion in layered porous media. Journal of the Hydraulic Division, 93(5), 237-260.

Sharma, H. D., and Reddy, K. R., 2004. Geoenvironmental engineering: Site remediation, waste containment, and emerging waste management technologies. Wiley, New York.

Shen, X., and Reible, D., 2015. An analytical solution for one-dimensional advective-dispersive solute equation in multilayered finite porous media. Transport in Porous Media, 107(3), 657-666.

Silva, O., Carrera, J., Dentz, M., Kumar, S., Alcolea, A., and Willmann, M., 2009. A general real-time formulation for multi-rate mass transfer problems. Hydrology and Earth System Sciences, 13, 1399-1411.

Sudicky, E. A. and McLaren, R. G., 1992. The Laplace Transform Galerkin Technique for large-scale simulation of mass transport in discretely fractured porous formations. Water Resources Research, 28(2), 499-514.

Taylor, G. I., 1953. Dispersion of soluble matter in solvent flowing through a tube. Proceedings of the Royal Society, A 219,186-203.

van Genuchten, M. T., 1985. Convective-dispersive transport of solutes involved in sequential first-order decay reactions. Computers & Geosciences, 11(2), 129-147.

van Genuchten, M. T. and Alves, W.J., 1982. Analytical solutions of the one-dimensional convective-dispersive solute transport equation, United States Department of Agriculture Technical Bulletins, 1661.

van Genuchten, M. T. and Alves, W.J., 1976. Mass transfer studies in sorbing porous media I. Analytical Solutions. Soil Science Society of America Journal, 40(4), 473-480.

van Genuchten, M. T. and Parker, J. C., 1984. Boundary conditions for displacement experiments through short laboratory soil columns. Soil Science Society of America Journal, 48, 703-708.

Wang, Q. and Zhan, H., 2015. On different numerical inverse Laplace methods for solute transport problems. Advances in Water Resources, 75, 80-92.

Wehner, J. F. and Wilhelm, R. H., 1956. Boundary conditions of flow reactor. Chemical Engineering Science, 6(2), 89-93.

Yeh, T. C. J., Khaleel, R., and Carroll, K. C., 2015. Flow through heterogeneous geologic media. Cambridge University Press, New York.

Zhang, X., 2002. Stochastic methods of flow in porous media. Elsevier Science, Netherlands.

Zheng, C. and Bennett, G. D., 1995. Applied contaminant transport modeling. Theory and practice. van Nonstrand-Reinhold, New York.

APPENDIX A

Calculation of coefficients *A, B, E, F.*

$$A + B - \frac{1}{P_{e1}}\left(-A\omega_1 - B\omega_2\right) = \frac{1}{s} \tag{A-1}$$

$$Ae^{-\omega_1 L_1} + Be^{-\omega_2 L_1} = Ee^{-\omega_3 L_1} + Fe^{-\omega_4 L_1} \tag{A-2}$$

$$-\omega_1 Ae^{-\omega_1 L_1} - \omega_2 Be^{-\omega_2 L_1} = -\gamma\beta\omega_3 Ee^{-\omega_3 L_1} - \gamma\beta\omega_4 Fe^{-\omega_4 L_1} \tag{A-3}$$

$$-\omega_3 Ee^{-\omega_3} - \omega_4 Fe^{-\omega_4} = 0 \tag{A-4}$$

From Eq. (A-1):

$$\mathrm{A} = \frac{P_{e1}}{s\left(P_{e1} + \omega_1\right)} - \frac{P_{e1} + \omega_2}{P_{e1} + \omega_1} B \tag{A-5}$$

From Eq. (A-4):

$$\mathrm{E} = -\frac{\omega_4 e^{-\omega_4}}{\omega_3 e^{-\omega_3}} F = -\frac{\omega_4}{\omega_3} e^{\omega_3 - \omega_4} F \tag{A-6}$$

Substituting the result of Eq. (A-5) and (A-6) into equation (A-2):

$$\left(\frac{P_{e1}}{s\left(P_{e1} + \omega_1\right)} - \frac{P_{e1} + \omega_2}{P_{e1} + \omega_1} B\right) e^{-\omega_1 L_1} + Be^{-\omega_2 L_1} = -\frac{\omega_4}{\omega_3} e^{\omega_3 - \omega_4} Fe^{-\omega_3 L_1} + Fe^{-\omega_4 L_1} \tag{A-7}$$

Then we obtain the result as below:

$$\mathrm{F} = \frac{\dfrac{P_{e1}}{s\left(P_{e1} + \omega_1\right)} e^{-\omega_1 L_1}}{e^{-\omega_4 L_1} - \dfrac{\omega_4}{\omega_3} e^{\omega_3 - \omega_4} e^{-\omega_3 L_1}} + \frac{e^{-\omega_2 L_1} - \dfrac{P_{e1} + \omega_2}{P_{e1} + \omega_1} e^{-\omega_1 L_1}}{e^{-\omega_4 L_1} - \dfrac{\omega_4}{\omega_3} e^{\omega_3 - \omega_4} e^{-\omega_3 L_1}} B \tag{A-8}$$

Substituting the result of Eq. (A-5) and (A-6) into equation (A-3):

$$-\omega_1\left(\frac{P_{e1}}{s\left(P_{e1}+\omega_1\right)}-\frac{P_{e1}+\omega_2}{P_{e1}+\omega_1}B\right)e^{-\omega_1 L_1}-\omega_2 Be^{-\omega_2 L_1}=-\gamma\beta\omega_3\left(-\frac{\omega_4}{\omega_3}e^{\omega_3-\omega_4}F\right)e^{-\omega_3 L_1}-\gamma\beta\omega_4 Fe^{-\omega_4 L_1} \quad \text{(A-9)}$$

The result comes out:

$$\mathrm{F}=\frac{-\omega_1 P_{e1}e^{-\omega_1 L_1}}{s\left(P_{e1}+\omega_1\right)\left(\gamma\beta\omega_3\frac{\omega_4}{\omega_3}e^{\omega_3-\omega_4}e^{-\omega_3 L_1}-\gamma\beta\omega_4 e^{-\omega_4 L_1}\right)}+\frac{\omega_1\frac{P_{e1}+\omega_2}{P_{e1}+\omega_1}e^{-\omega_1 L_1}-\omega_2 e^{-\omega_2 L_1}}{\gamma\beta\omega_3\frac{\omega_4}{\omega_3}e^{\omega_3-\omega_4}e^{-\omega_3 L_1}-\gamma\beta\omega_4 e^{-\omega_4 L_1}}B \quad \text{(A-10)}$$

According to Eq. (A-9) and (A-10):

$$\begin{aligned}&\frac{-\omega_1 P_{e1}e^{-\omega_1 L_1}}{s\left(P_{e1}+\omega_1\right)\left(\gamma\beta\omega_3\frac{\omega_4}{\omega_3}e^{\omega_3-\omega_4}e^{-\omega_3 L_1}-\gamma\beta\omega_4 e^{-\omega_4 L_1}\right)}+\frac{\omega_1\frac{P_{e1}+\omega_2}{P_{e1}+\omega_1}e^{-\omega_1 L_1}-\omega_2 e^{-\omega_2 L_1}}{\gamma\beta\omega_3\frac{\omega_4}{\omega_3}e^{\omega_3-\omega_4}e^{-\omega_3 L_1}-\gamma\beta\omega_4 e^{-\omega_4 L_1}}B \\ &=\frac{\frac{P_{e1}}{s\left(P_{e1}+\omega_1\right)}e^{-\omega_1 L_1}}{e^{-\omega_4 L_1}-\frac{\omega_4}{\omega_3}e^{\omega_3-\omega_4}e^{-\omega_3 L_1}}+\frac{e^{-\omega_2 L_1}-\frac{P_{e1}+\omega_2}{P_{e1}+\omega_1}e^{-\omega_1 L_1}}{e^{-\omega_4 L_1}-\frac{\omega_4}{\omega_3}e^{\omega_3-\omega_4}e^{-\omega_3 L_1}}B\end{aligned} \quad \text{(A-11)}$$

Then we obtain the result:

$$\mathrm{B}=\frac{\frac{-\omega_1 P_{e1}e^{-\omega_1 L_1}}{s\left(P_{e1}+\omega_1\right)\left(\gamma\beta\omega_3\frac{\omega_4}{\omega_3}e^{\omega_3-\omega_4}e^{-\omega_3 L_1}-\gamma\beta\omega_4 e^{-\omega_4 L_1}\right)}-\frac{\frac{P_{e1}}{s\left(P_{e1}+\omega_1\right)}e^{-\omega_1 L_1}}{e^{-\omega_4 L_1}-\frac{\omega_4}{\omega_3}e^{\omega_3-\omega_4}e^{-\omega_3 L_1}}}{\frac{e^{-\omega_2 L_1}-\frac{P_{e1}+\omega_2}{P_{e1}+\omega_1}e^{-\omega_1 L_1}}{e^{-\omega_4 L_1}-\frac{\omega_4}{\omega_3}e^{\omega_3-\omega_4}e^{-\omega_3 L_1}}-\frac{\omega_1\frac{P_{e1}+\omega_2}{P_{e1}+\omega_1}e^{-\omega_1 L_1}-\omega_2 e^{-\omega_2 L_1}}{\gamma\beta\omega_3\frac{\omega_4}{\omega_3}e^{\omega_3-\omega_4}e^{-\omega_3 L_1}-\gamma\beta\omega_4 e^{-\omega_4 L_1}}} \quad \text{(A-12)}$$

Set up $e^{\omega_3-\omega_4}=\alpha,\ e^{\omega_1-\omega_2}=\delta$

Then the final solution comes out:

$$\mathrm{B}=\frac{P_{e1}}{s}\frac{\omega_1\left(\omega_3\alpha^{L_1}-\omega_4\alpha\right)+\gamma\beta\omega_4\omega_3\left(\alpha-\alpha^{L_1}\right)}{\gamma\beta\omega_3\omega_4\left(\alpha-\alpha^{L_1}\right)\left(\omega_2\delta^{L_1}-\omega_1\right)+\left(\omega_3\alpha^{L_1}-\omega_4\alpha\right)\left(-\omega_1^{\ 2}+\omega_2^{\ 2}\delta^{L_1}\right)} \quad \text{(A-13)}$$

From Eq. (A-5), (A-6), (A-8) and (A-13), A, E, F could be found.

APPENDIX B

1. MATLAB script for the Laplace transform of concentration in the first zone

```
%solution for concentration of zone 1
%convection in the p-domain
%
function[F]=concen3(p,x,Pe1,Pe2,L1,lamedh1,lamedh2,R1,R2,beta)

omega1=-Pe1*0.5+0.5*sqrt(Pe1^2+4*(lamedh1+p)*R1);
omega2=-Pe1*0.5-0.5*sqrt(Pe1^2+4*(lamedh1+p)*R1);
omega3=-Pe2*0.5+0.5*sqrt(Pe2^2+4*(lamedh2+p/beta)*R2);
omega4=-Pe2*0.5-0.5*sqrt(Pe2^2+4*(lamedh2+p/beta)*R2);

F=(-Pe1./(p.*omega2)).*exp(-omega1.*x)-(omega1./omega2.*exp(-omega1*x)).*(Pe1.*exp((omega2-
omega1)*L1).* ...
((omega1.*omega3.*exp((omega3-omega4).*(L1-1))-omega1.*omega4)+(beta.*omega3.*omega4.*(1-exp((omega3-
omega4).*(L1-1))))./ ...
(p.*((beta.*omega3.*omega4.*(1-exp((omega3-omega4).*(L1-1))).*(omega2-omega1.*exp((omega2-
omega1).*L1)))+((omega3.*exp((omega3-omega4) ...
*(L1-1))-omega4).*(-(omega1.^2).*(exp((omega2-omega1)*L1))+omega2.^2)))))+exp(-omega1*L1).*exp(-
omega2.*(x-L1)).*Pe1.* ...
((omega1.*omega3.*exp((omega3-omega4).*(L1-1))-omega1.*omega4)+(beta.*omega3.*omega4.*(1-exp((omega3-
omega4).*(L1-1))))./ ...
(p.*((beta.*omega3.*omega4.*(1-exp((omega3-omega4).*(L1-1))).*(omega2-omega1.*exp((omega2-
omega1).*L1)))+((omega3.*exp((omega3-omega4)*(L1-1))-omega4).*(-(omega1.^2).*(exp((omega2-
omega1)*L1))+omega2.^2))));
end
```

2. MATLAB script for the Laplace transform of concentration in the second zone

```
%solution for concentration of zone 2
%convection in the p-domain
%
function[F]=concen4(p,x,Pe1,Pe2,L1,lamedh1,lamedh2,R1,R2,beta)

omega1=-Pe1*0.5+0.5*sqrt(Pe1^2+4*(lamedh1+p)*R1);
omega2=-Pe1*0.5-0.5*sqrt(Pe1^2+4*(lamedh1+p)*R1);
omega3=-Pe2*0.5+0.5*sqrt(Pe2^2+4*(lamedh2+p/beta)*R2);
omega4=-Pe2*0.5-0.5*sqrt(Pe2^2+4*(lamedh2+p/beta)*R2);

F=-(-Pe1.*omega4.*exp(omega3*(L1-1)-omega1*L1+omega4)./(p.*omega2.*(omega3.*exp((omega3-omega4).*(L1-
2))-omega4.*exp(omega4-omega3))) ...
   -(exp(omega3*(L1-1)-omega1*L1+omega4)-omega1./omega2.*exp(omega3*(L1-1)-
omega1*L1+omega4).*exp((omega2-omega1)*L1))./ ...
   (omega3./omega4.*exp((omega3-omega4).*(L1-2))-exp(omega4-
omega3)).*(Pe1.*((omega1.*omega3.*exp((omega3-omega4).*(L1-1))-omega1.*omega4) ...
   +(beta.*omega3.*omega4.*(1-exp((omega3-omega4).*(L1-1))))./(p.*((beta.*omega3.*omega4.*(1-exp((omega3-
omega4).*(L1-1))).* ...
   (omega2-omega1.*exp((omega2-omega1).*L1)))+((omega3.*exp((omega3-omega4)*(L1-1))-omega4).*(-
(omega1.^2).*(exp((omega2-omega1)*L1))+omega2.^2)))))).*exp(-omega3.*x)- ...
   Pe1.*omega3.*exp(omega3*(L1-1)-omega1*L1)./(p.*omega2.*(omega3.*exp((omega3-omega4).*(L1-1))-
omega4)).*exp(-omega4.*(x-1)) ...
   +exp(omega3*(L1-1)-omega1*L1).*(1-omega1./omega2.*exp((omega2-omega1)*L1))./(exp((omega3-
omega4)*(L1-1))-omega4./omega3).* ...
   (Pe1.*((omega1.*omega3.*exp((omega3-omega4).*(L1-1))-omega1.*omega4)+(beta.*omega3.*omega4.*(1-
exp((omega3-omega4).*(L1-1))))./ ...
   (p.*((beta.*omega3.*omega4.*(1-exp((omega3-omega4).*(L1-1))).*(omega2-omega1.*exp((omega2-
omega1).*L1)))+((omega3.*exp((omega3-omega4)*(L1-1))-omega4).* ...
   (-(omega1.^2).*(exp((omega2-omega1)*L1))+omega2.^2))))).*exp(-omega4.*(x-1));
end
```

3. MATLAB script for breakthrough curve

```
clc;
clear;

a=linspace(1,150,1001)';  % times to evaluate solution
q=2;                      % q to Darcy velocity
pro1=0.5;                 % porosity of zone 1
pro2=0.5;                 % porosity of zone 2
alpha1=3;                 % dispersivity of zone 1
alpha2=2;                 % dispersivity of zone 2
v1=q/pro1;                % velocity of zone1
v2=q/pro2;                % velocity of zone2
D1=v1*alpha1;             % dispersion coefficient of zone1
D2=v2*alpha2;             % dispersion coefficient of zone2

L=100;                    % total zone length
L1=90/L;                  % relative length of zone 1
lamedh1=0.02*L^2/D1;
lamedh2=0.01*L^2/D2;
R1=1.5;
R2=2;

Pe1=v1*L/D1;
Pe2=v2*L/D2;
beta=D2/D1;


t=D1/L^2*a;

tol1=0;  % default for largest pole for function
tol=1e-9;  % default for numerical tolerance of approaching pole
%invert Laplace transform
x=100/L;  % position (m)

T=invlap('concen5',t,tol1,tol,x,Pe1,Pe2,L1,lamedh1,lamedh2,R1,R2,beta);



plot(a,T)
ylim([0 1])
%xlim([0 100])
xlabel('t')
ylabel('C/Co')
```

4. MATLAB script for curve fitting function

```
function [par,RMSE]=fit(par0,a,ydata)
   [par1,resnorm,residual] = lsqcurvefit(@fun,par0,a,ydata);
   par=par1;
   RMSE=sqrt(mean(residual.^2));
end

function Val=fun(par,a)
v=par(1);
D=par(2);
L=100;
L1=100/L;
lamedh1=0.000*L^2/D;
lamedh2=0.000*L^2/D;
R1=1;
R2=1;
Pe1=v*L/D;
Pe2=v*L/D;
beta=D/D;
t=D/L^2*a;
tol1=0;  % default for largest pole for function
tol=1e-9;  % default for numerical tolerance of approaching pole
%invert Laplace transform
x=100/L;  % position (m)
Val=invlap('concen3',t,tol1,tol,x,Pe1,Pe2,L1,lamedh1,lamedh2,R1,R2,beta);
end
```

5. MATLAB script for coefficient solving by curve fitting function

```
clc;
clear;

a=linspace(1,150,1001)';
[ydata]=xlsread('C:\Users\Yang\Desktop\Book2.xlsx',5,'C1:C1001');
par0(1)=2;
par0(2)=3;
[par,RMSE]=fit(par0,a,ydata);


v=par(1);
D=par(2);
L=100;
L1=100/L;
lamedh1=0.000*L^2/D;
lamedh2=0.000*L^2/D;
R1=1;
R2=1;
Pe1=v*L/D;
Pe2=v*L/D;
beta=D/D;
t=D/L^2*a;
tol1=0;  % default for largest pole for function
tol=1e-9;  % default for numerical tolerance of approaching pole
%invert Laplace transform
x=100/L;  % position (m)
Val=invlap('concen3',t,tol1,tol,x,Pe1,Pe2,L1,lamedh1,lamedh2,R1,R2,beta);
plot(a,Val,a,ydata);
legend('fit curve','case7')
ylim([0 1])
v
D
RMSE
```